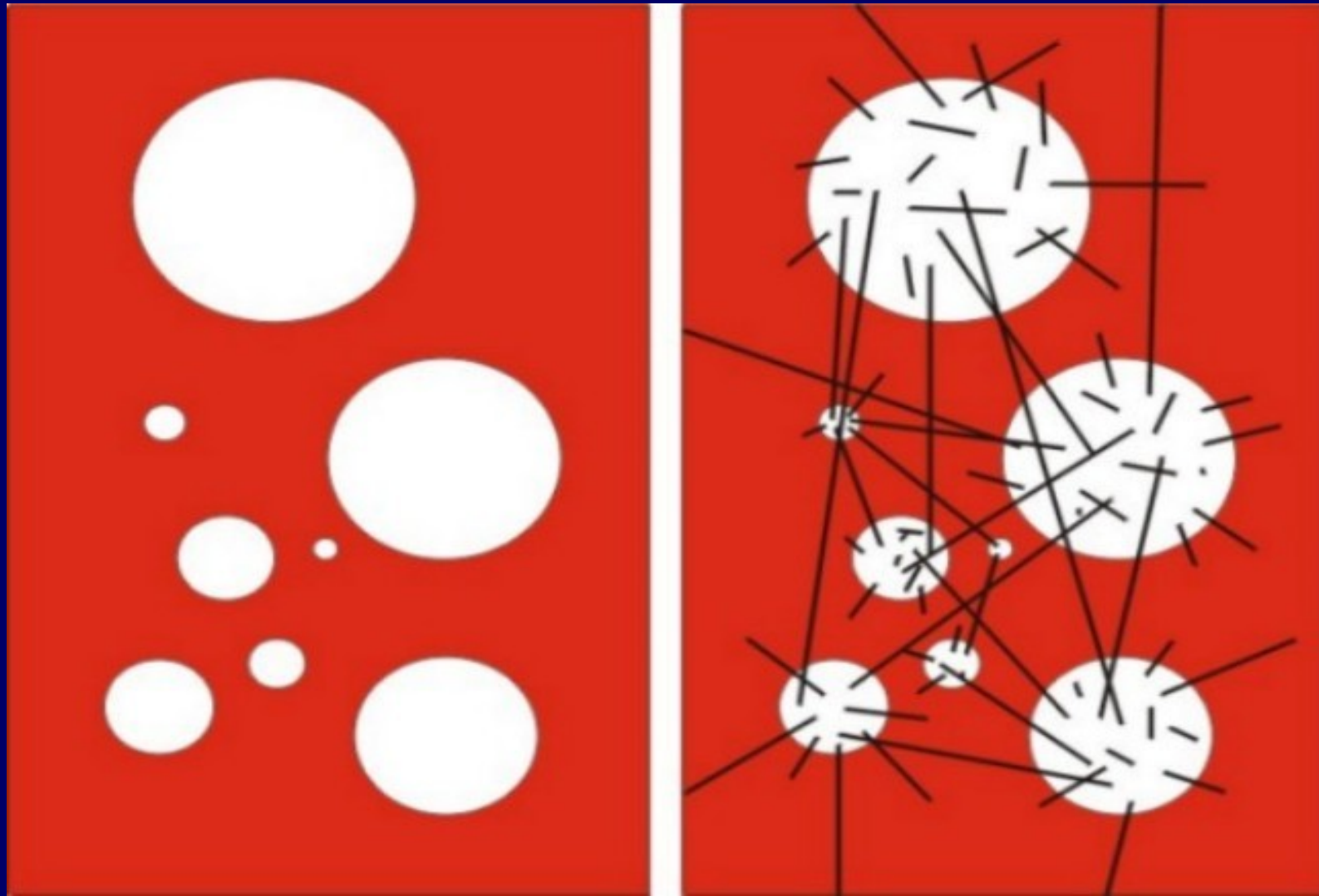


«Multiverse» («Многомир») и первичные магнитные кротовые норы.

Пущино, 24 апреля 2008.



Отличия КН от ЧД

1. Для входа в КН нет горизонта событий.
2. Возможны массы меньше звёздных.
3. Возможны нулевые и даже отрицательные массы.
4. Излучение и частицы проходят в обе стороны.
5. Красное и синее смещение.
6. Сквозное и внешнее гравитационное линзирование.
7. Периодические радиальные орбиты.
8. Радиальное магнитное поле, может доминировать и на больших расстояниях.
9. Дипольное электрическое поле при вращении (односторонние выбросы, структура выбросов).
10. Нет эффекта Хокинга (магнитные ЧД и монополи).
11. Двойные системы входов (магнито-дипольное излучение, гравитац. излучение, слияние, γ -всплески).
12. Космологическая эволюция с ПКН и ПЧД.

Для $R \gg R_0$

$$H = G^{0.5} M / R^2.$$

Если $M = 3 \times 10^9 M_{\odot}$

и $R = 10$ кпс,

то $H = 1.5 \times 10^{-6}$ Гс.

Параметры магнитных кротовых нор

$2M_0$ (г)	r_0 (см)	H_0 (Гс)	ρ_0 (г/см ³)	v_G (Гц)	v_c (Гц)	v_H (Гц)
1	2	3	4	5	6	7
$6 \cdot 10^{42}$ ($= 3 \cdot 10^9 M_{\odot}$) квазар	$4.5 \cdot 10^{14}$	$7.8 \cdot 10^9$	$2.7 \cdot 10^{-3}$	$7.6 \cdot 10^{-6}$ (1.5 дня)	$1.2 \cdot 10^{-6}$ (10 дней)	$2.2 \cdot 10^{16}$
10^{39} ($= 5 \cdot 10^5 M_{\odot}$) рождение пар e^{\pm}	$7.4 \cdot 10^{10}$	$4.4 \cdot 10^{13}$	$9.7 \cdot 10^4$	0.045 (22 сек)	$6.9 \cdot 10^{-3}$ (2.4 мин)	$1.3 \cdot 10^{20}$
$2 \cdot 10^{33}$ ($= 1 M_{\odot}$) Солнце	$1.5 \cdot 10^5$	$2.3 \cdot 10^{19}$	$2.4 \cdot 10^{16}$	$2.3 \cdot 10^4$	$3.5 \cdot 10^3$	$6.6 \cdot 10^{25}$
$6 \cdot 10^{27}$ ($= 1 M_{\odot}$) Земля	0.45	$7.8 \cdot 10^{24}$	$2.7 \cdot 10^{27}$	$7.6 \cdot 10^9$	$1.2 \cdot 10^9$	$2.2 \cdot 10^{31}$
$5 \cdot 10^{10}$ позитроний	$3.5 \cdot 10^{-18}$	10^{42}	$4.4 \cdot 10^{61}$	$9.7 \cdot 10^{26}$	$1.5 \cdot 10^{26}$	$2.7 \cdot 10^{48}$
$1.8 \cdot 10^3$ рождение пар μ^{\pm}	$1.3 \cdot 10^{-25}$	$2.6 \cdot 10^{49}$	$3.0 \cdot 10^{76}$	$2.6 \cdot 10^{34}$	$4.0 \cdot 10^{33}$	$7.3 \cdot 10^{55}$
$2 \cdot 10^{-5}$ Планковская масса	$1.5 \cdot 10^{-33}$	$2.3 \cdot 10^{57}$	$2.4 \cdot 10^{92}$	$2.3 \cdot 10^{42}$	$3.5 \cdot 10^{41}$	$6.6 \cdot 10^{63}$

Patrick Dineen, Peter Coles,

A Faraday Rotation Template
for the Galactic Sky, MNRAS,
362 (2005) 403-410;

astro-ph/0410636 v2

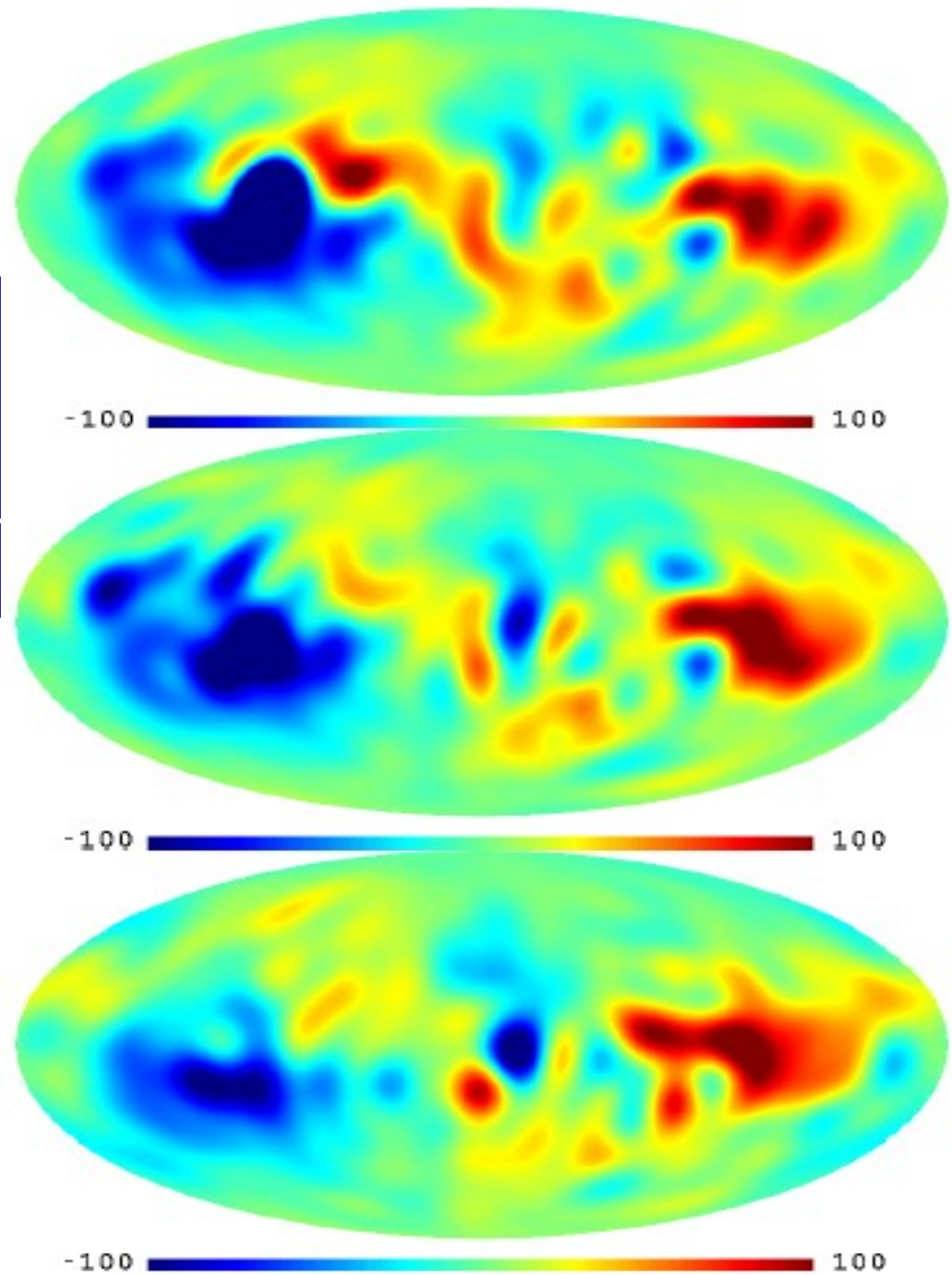


Figure 5. RM maps with identical temperature-colour scaling ($l_{\max} = 16$). From top to bottom: S81, B88 and F01 catalogues.

astro-ph/0601357, Pulsar rotation measures and the large-scale structure of Galactic magnetic field

J.L. Han, R.N. Manchester, A.G. Lyne, G.J. Qiao, W. van Straten

, *Astrophys.J.* 642, 868-881, 2006.

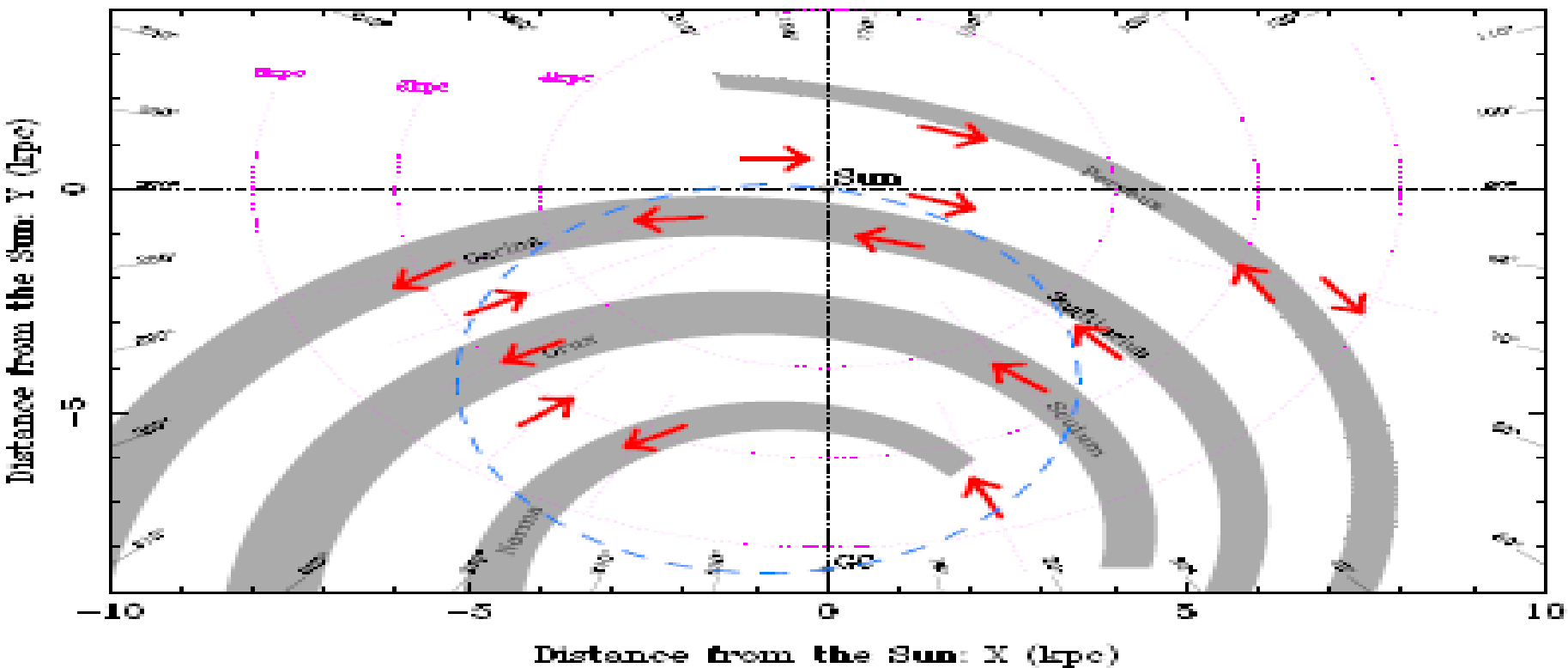


FIG. 12.— Global pattern of magnetic field directions inferred from RM–DM fits to the pulsar data and assuming an overall spiral pattern for the large-scale field. Field directions in the local region ($< 3\text{ kpc}$ from the Sun) and in the Perseus arm were taken from previous studies (e.g. Han & Qiao 1994; Indrani & Deshpande 1998) (see text). The dashed circle is the locus of tangential points for equiangular spirals of pitch angle -11° .

A.Fletcher et al., A&A, 414, 53-67 (2004)

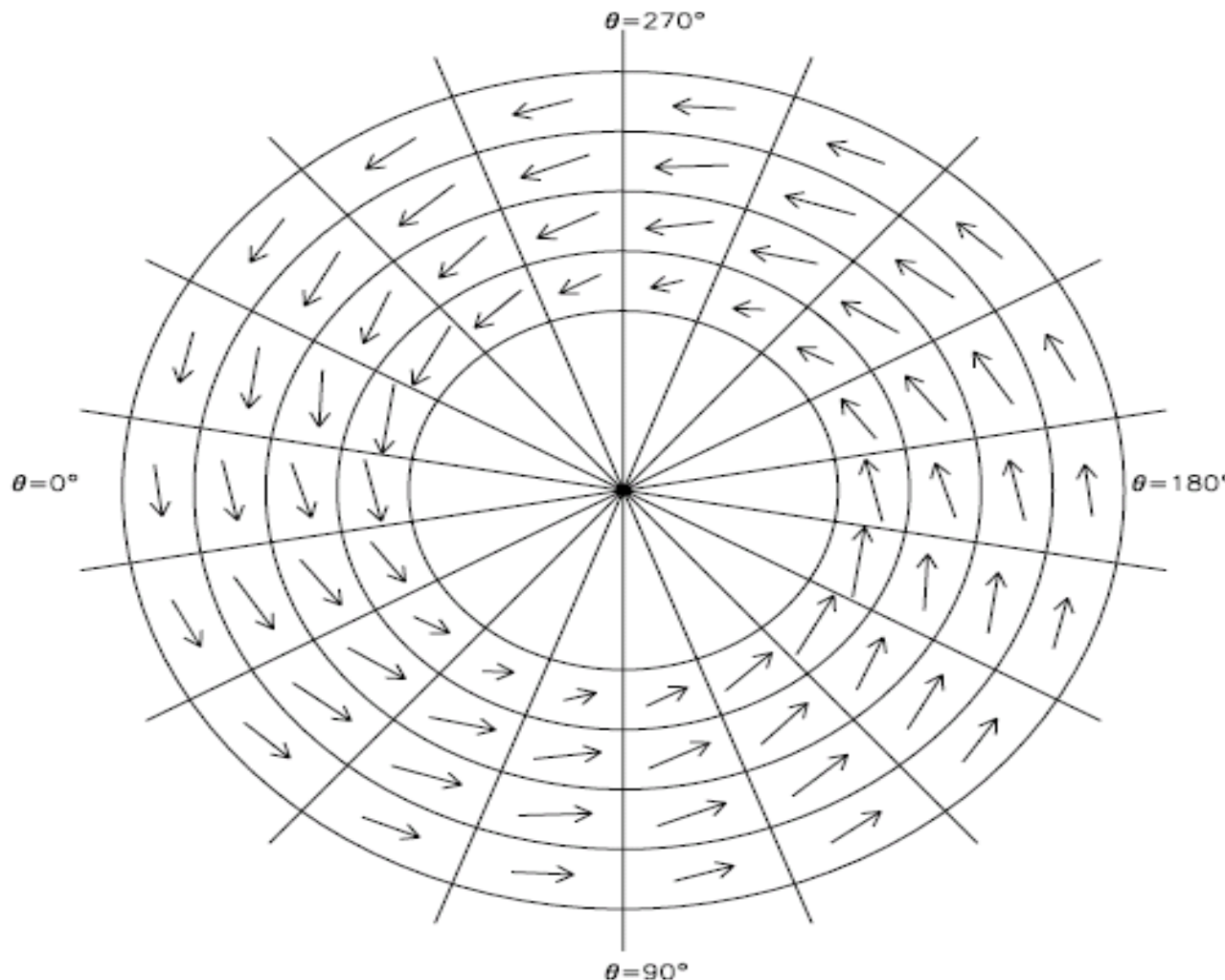


Fig. 6. Face-on view of M31 showing sectors and regular magnetic field vectors obtained from the fits shown in Table 2. The grid radii are 6, 8, 10, 12 and 14 kpc. The length of the vectors is proportional to B .

Germany.
Edited by The Regular Magnetic Fields of M 31 and M 33,
Elly M.
Berkhuijse

From Radio Polarization Observations

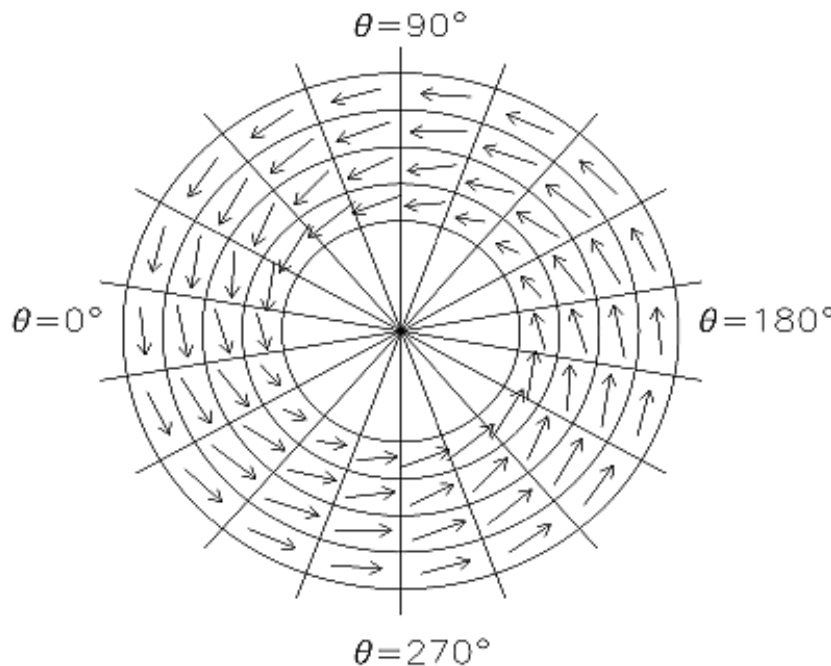
n, Rainer Andrew Fletcher¹, Rainer Beck², Elly M. Berkhuijsen², Anvar Shukurov¹

Beck,

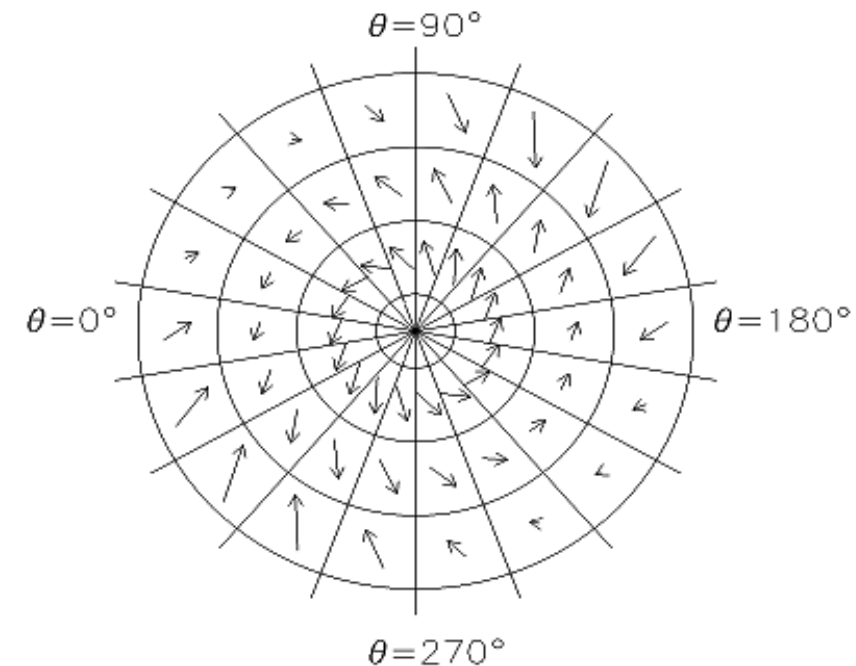
and Rene

A. M.

Walterbos.

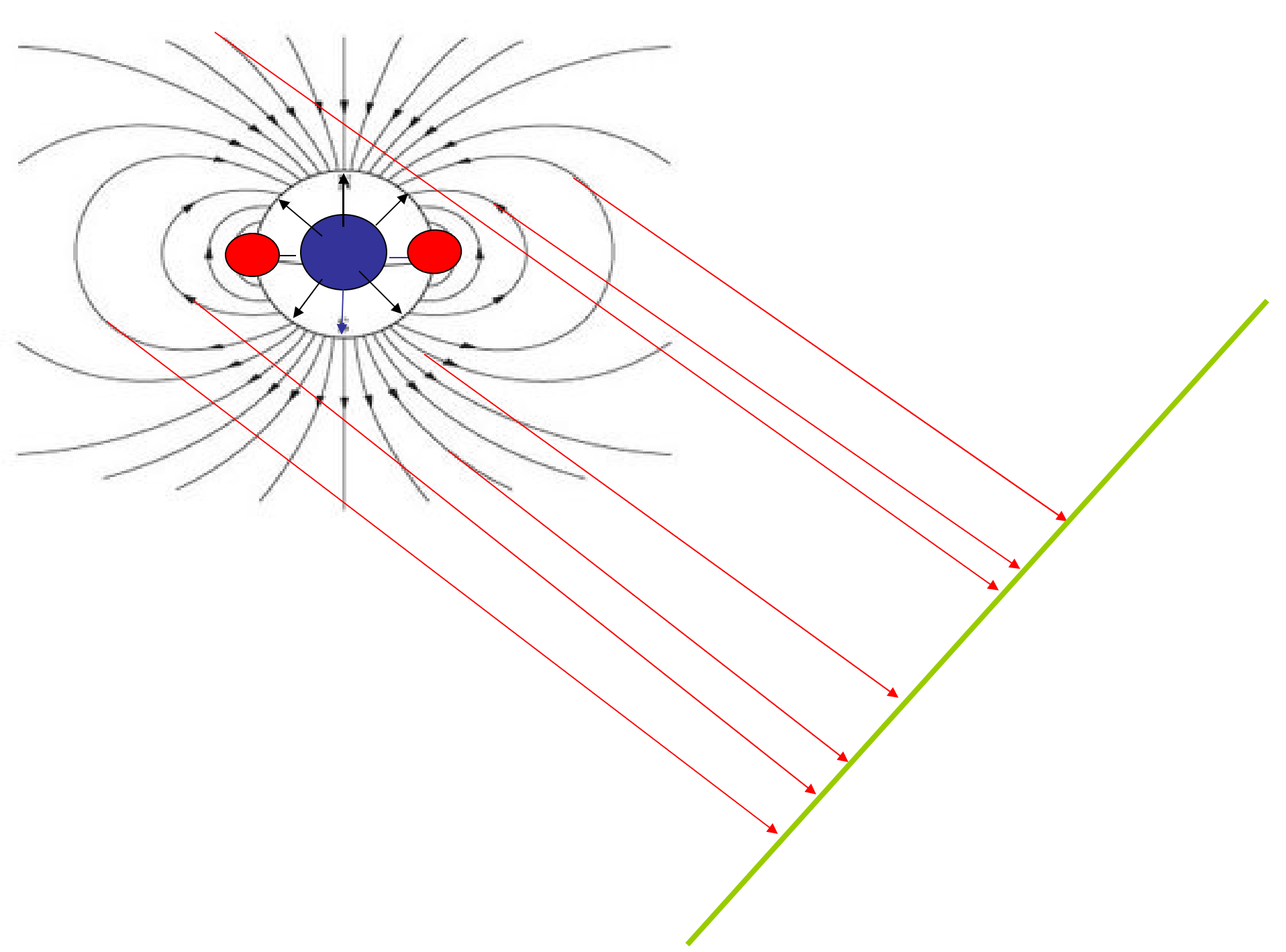


(a) M 31.



(b) M 33.

Fig. 1. Face-on view of galaxies showing sectors and regular magnetic field vectors obtained from the fits. The grid radii are 6, 8, 10, 12 and 14 kpc in M 31 and 1, 3, 5 and 7 kpc in M 33. The length of the vectors is proportional to \mathbf{B} .



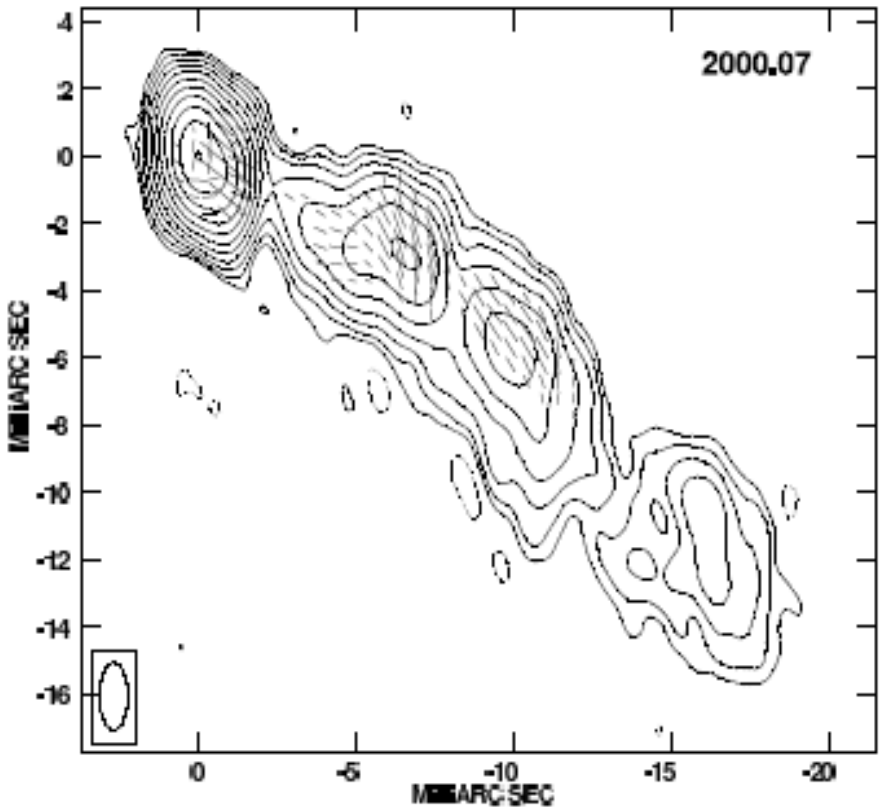
Faraday Rotation Measure Gradients from a Helical Magnetic Field in 3C 273

R.T. Zavala¹ and G.B. Taylor^{2,3}

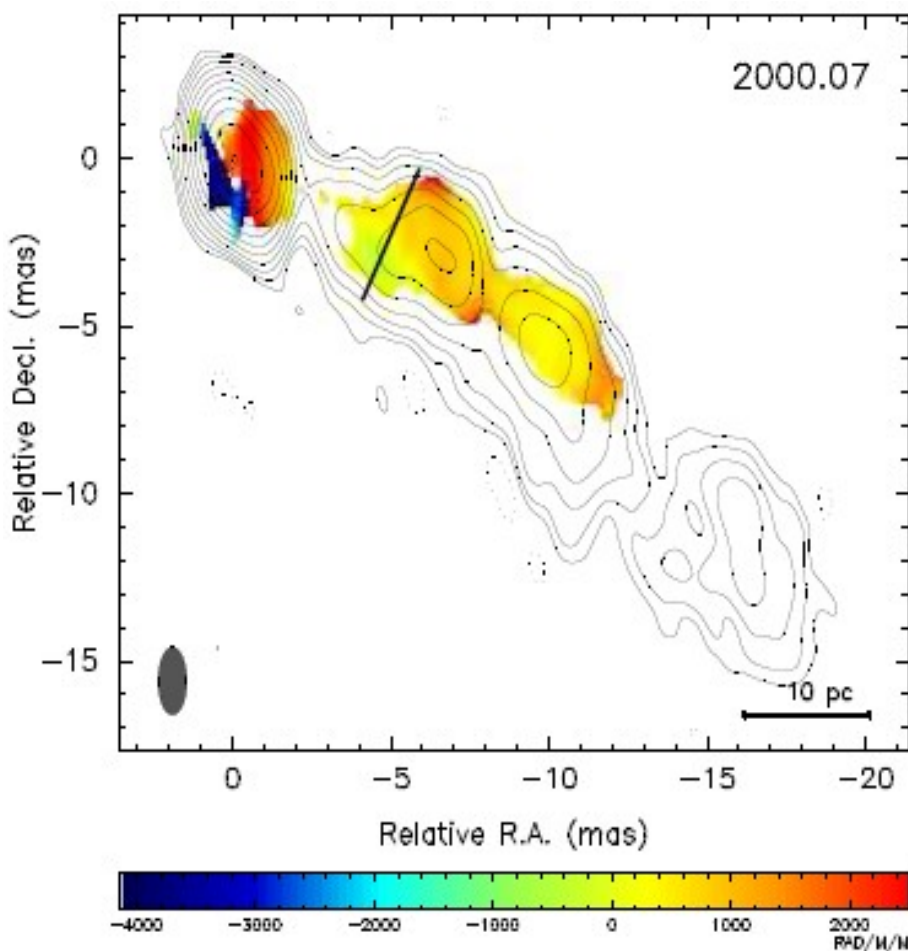
bzavala@nofs.navy.mil; gtaylor@nrao.edu

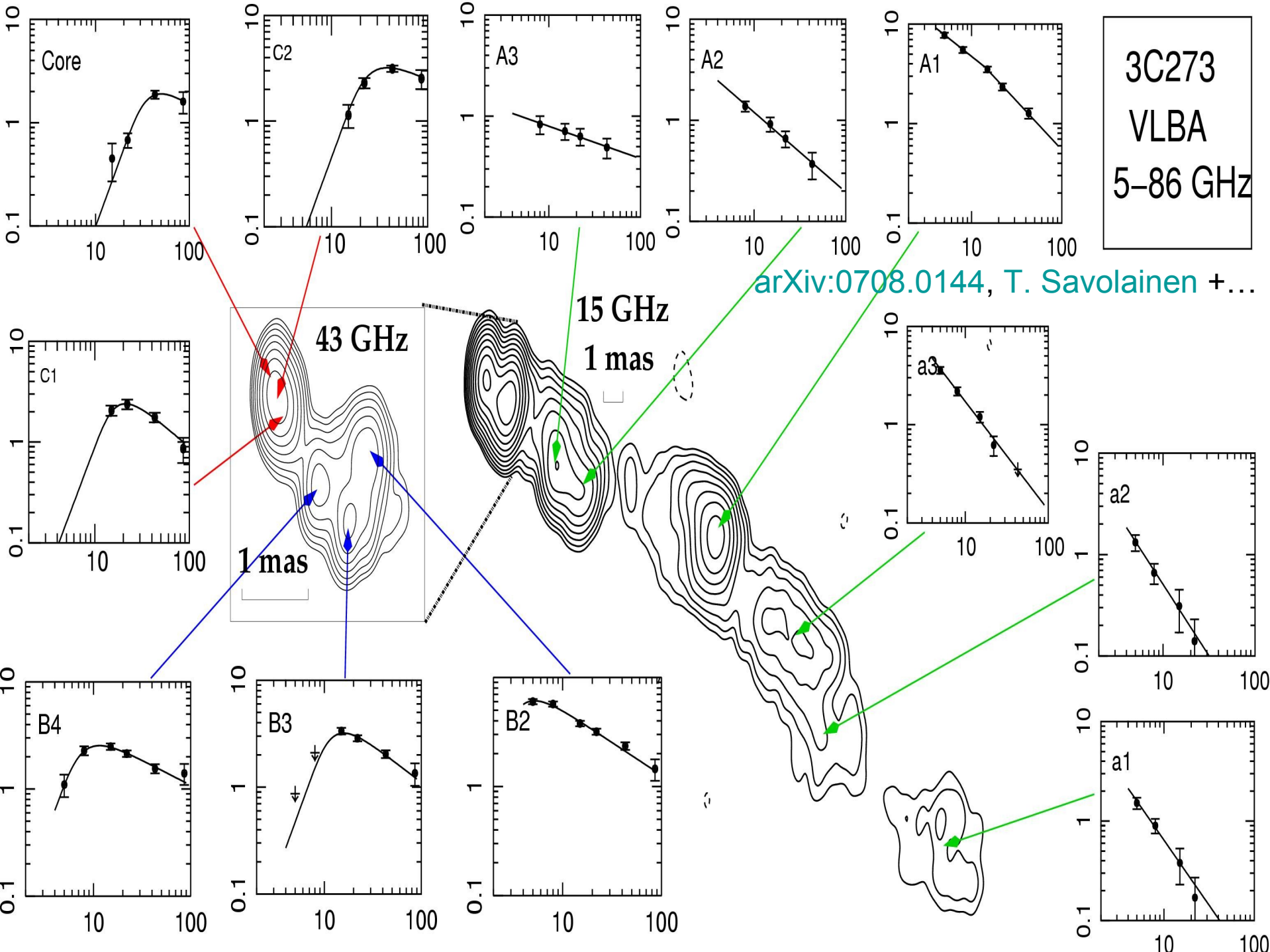
ABSTRACT

Using high frequency (12-22 GHz) VLBA observations we confirm the existence of a Faraday rotation measure gradient of $\sim 500 \text{ rad m}^{-2} \text{ mas}^{-1}$ transverse to the jet axis in the quasar 3C 273. The gradient is seen in two epochs spaced roughly six months apart. This stable transverse rotation measure gradient is expected if a helical magnetic field wraps around the jet. The overall order to the magnetic field in the inner projected 40 parsecs is consistent with a helical field. However, we find an unexpected increase in fractional polarization along the edges of the source, contrary to expectations. This high fractional polarization rules out internal Faraday rotation, but is not readily explained by a helical field. After correcting for the rotation measure, the intrinsic magnetic field direction in the jet of 3C 273 changes from parallel to nearly perpendicular to the projected jet motion at two locations. If a helical magnetic field causes the observed rotation measure gradient then the synchrotron emitting electrons must be separate from the helical field region. The presence or absence of transverse rotation measure gradients in other sources is also discussed.



3C273





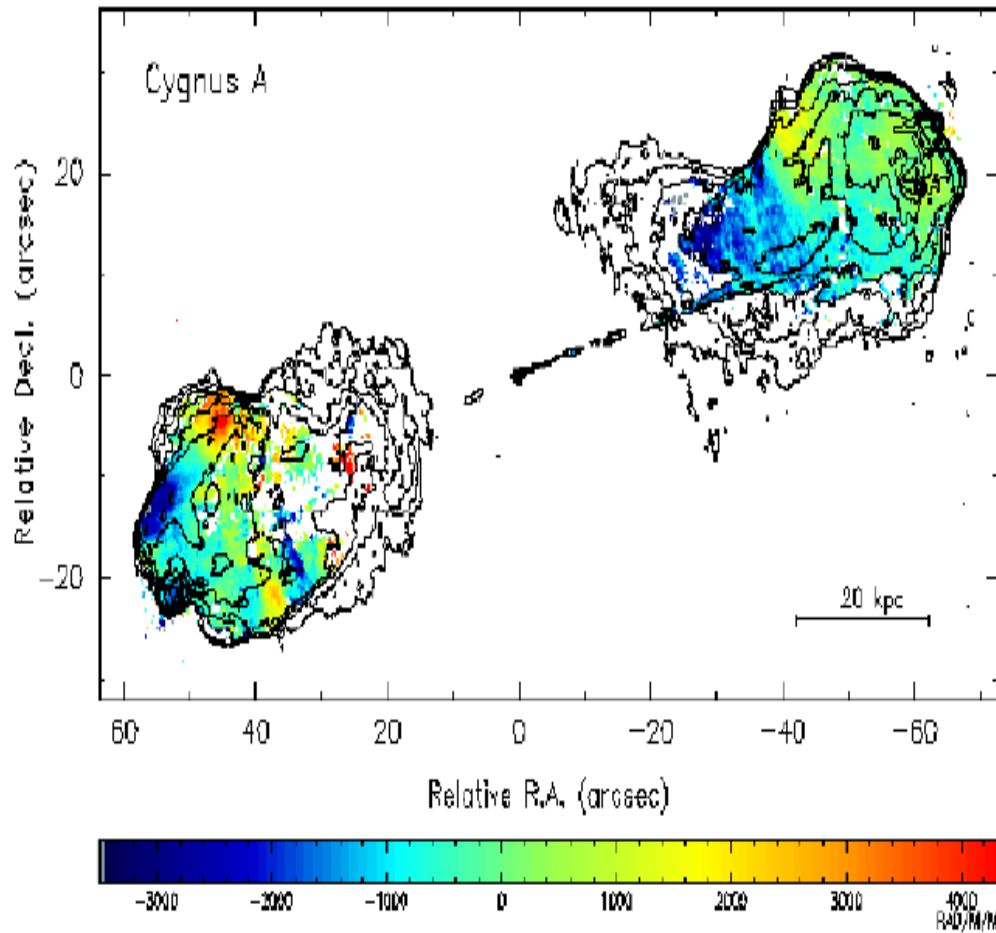


Figure 2: The RM distribution in Cygnus A based on multi-frequency, multi-configuration VLA observations. The resolution is $0.35''$ (Dreher et al. 1987). The colorbar indicates the range in RMs from -3400 to $+4300$ rad m⁻². Note the undulations in RM on scales of 10–30 kpc. Contours are overlaid from a 5 GHz total intensity image. The RM was solved for by fitting for the change in polarization angle with frequency on a pixel-by-pixel basis (see Fig. 5).

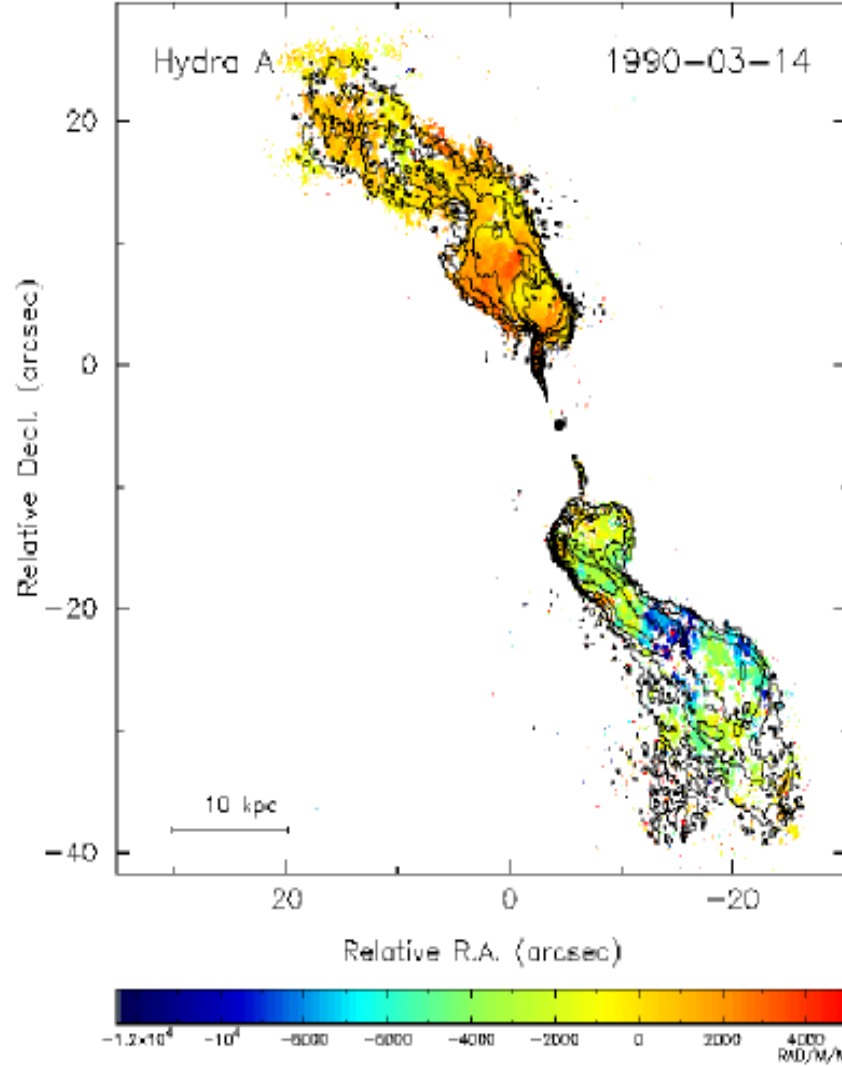


Figure 4: The RM distribution in Hydra A at a resolution of $0.3''$ (Taylor & Perley 1993) with total intensity contours overlaid. Multi-configuration VLA observations were taken at 4 widely spaced frequencies within the 8.4 GHz band, and a single frequency in the 15 GHz band. The colorbar indicates the range in RMs from -12000 to $+5000$ rad m⁻².

A View through Faraday's Fog: Parsec-Scale Rotation Measures in Active Galactic Nuclei, [Zavala, R. T.; Taylor, G. B.](#),
The Astrophysical Journal, V. 589, pp. 126-146, 2003.
Q B2005+403, z=1.74, F₁₅=2.51 Jy.

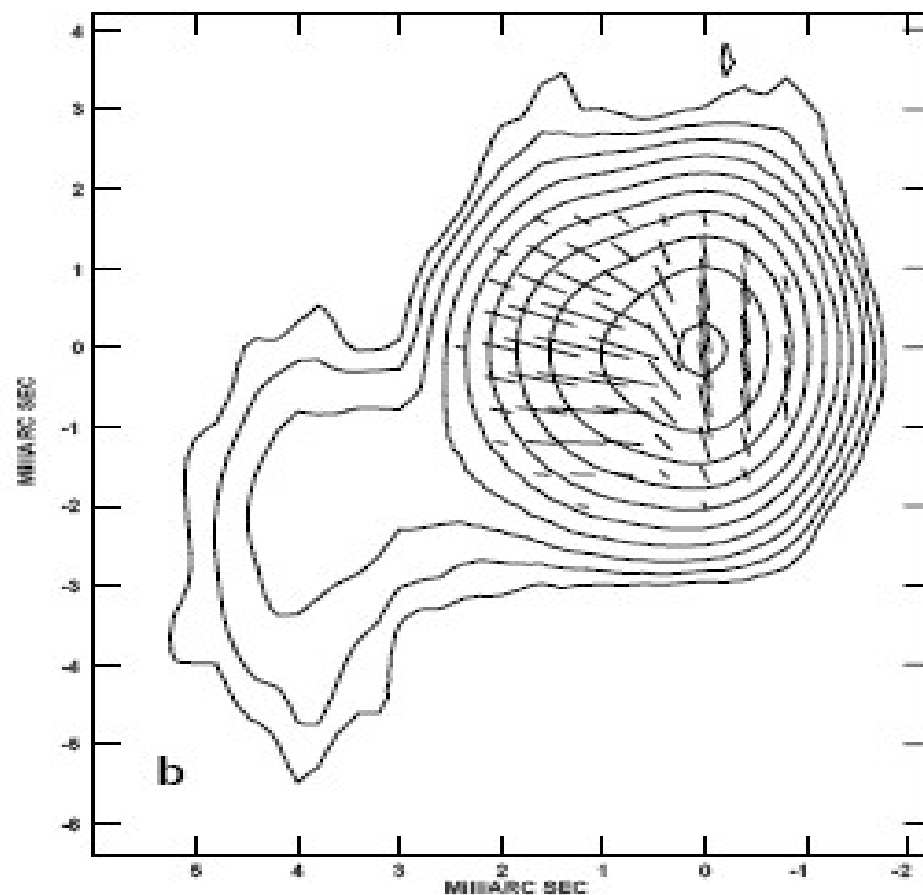
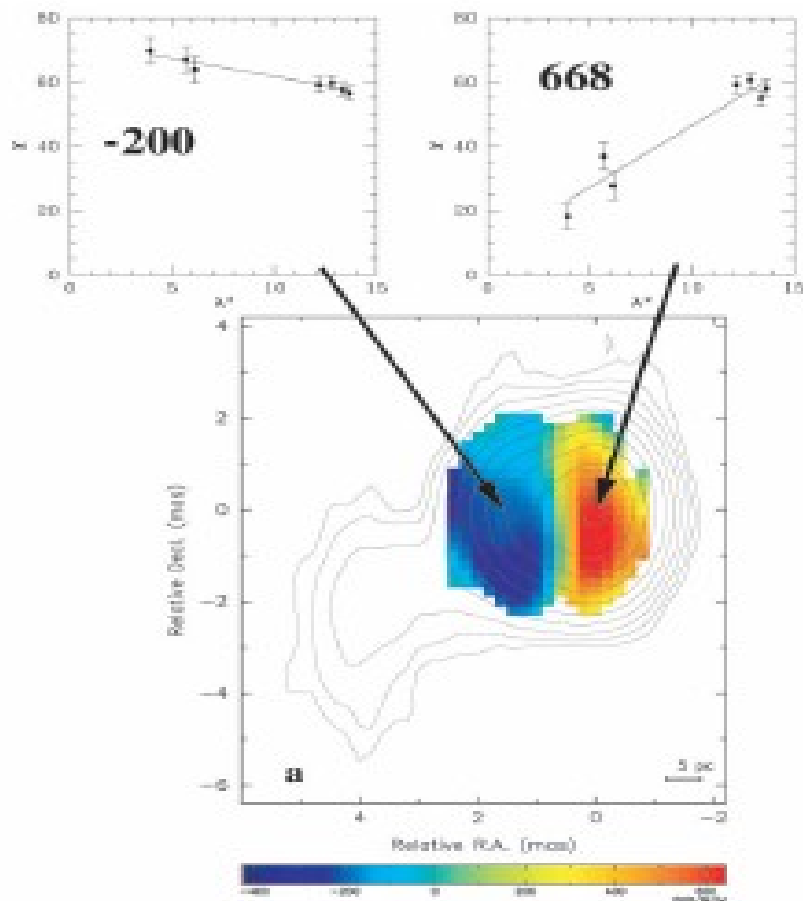


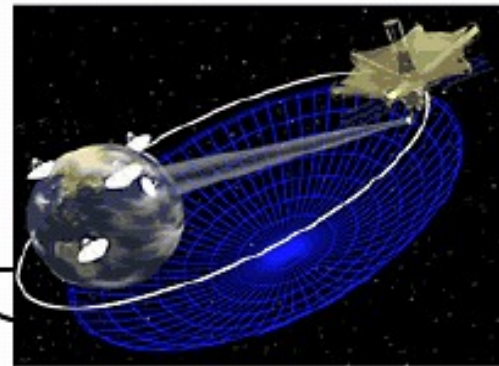
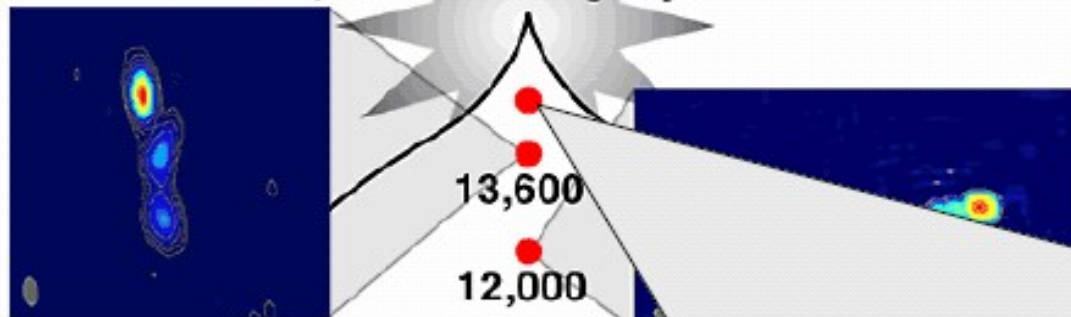
FIG. 23.—(a) RM image (color) for B2005+403 overlaid on Stokes I contours at 15 GHz. The insets show plots of EVPA χ (degrees) vs. λ^2 (units of cm $^{-3}$ s). (b) Electric vectors r_s (1 mas = 20 mJy beam $^{-1}$ polarized flux density) corrected for Faraday rotation overlaid on Stokes I contours. Contours start at 2.5 mJy beam $^{-1}$ and increase by factors of 2.

**These were the most
distant objects
targeted with VSOP**

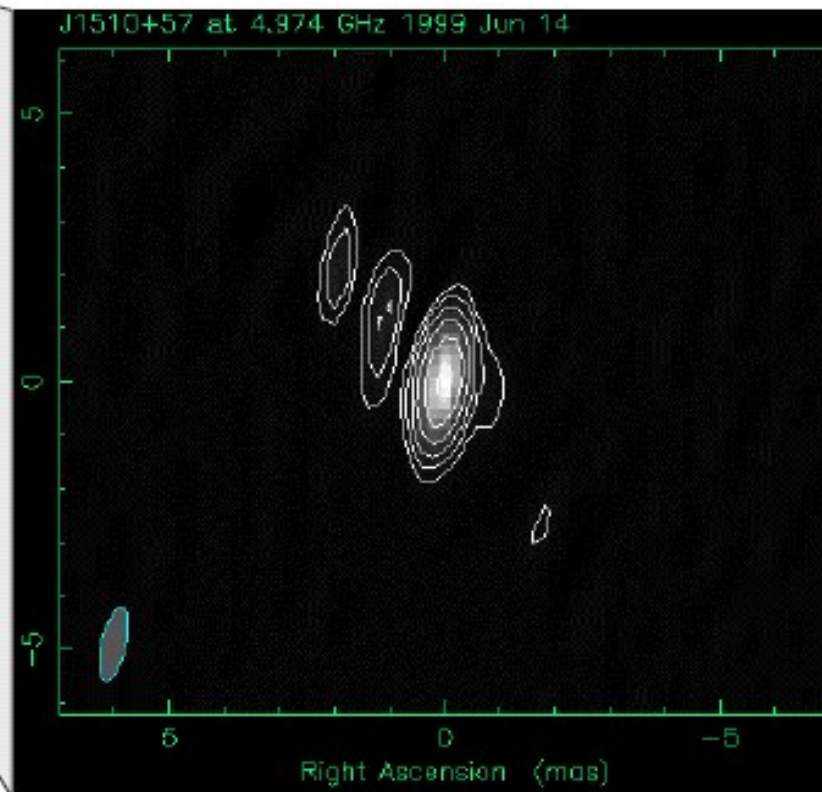
VSOP IMAGES

BIG BANG

15,000 million light years



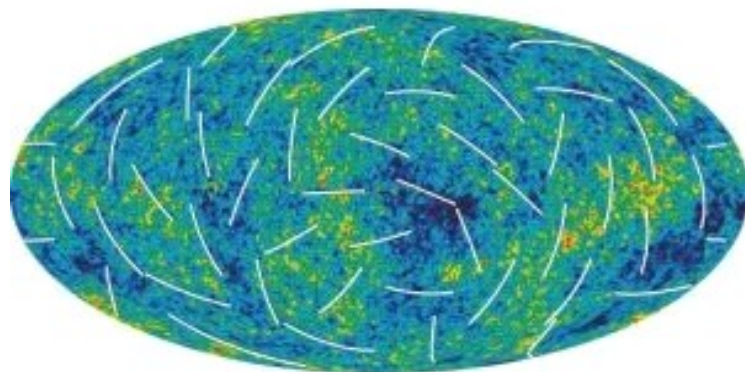
1508+572
 $z = 4.30$



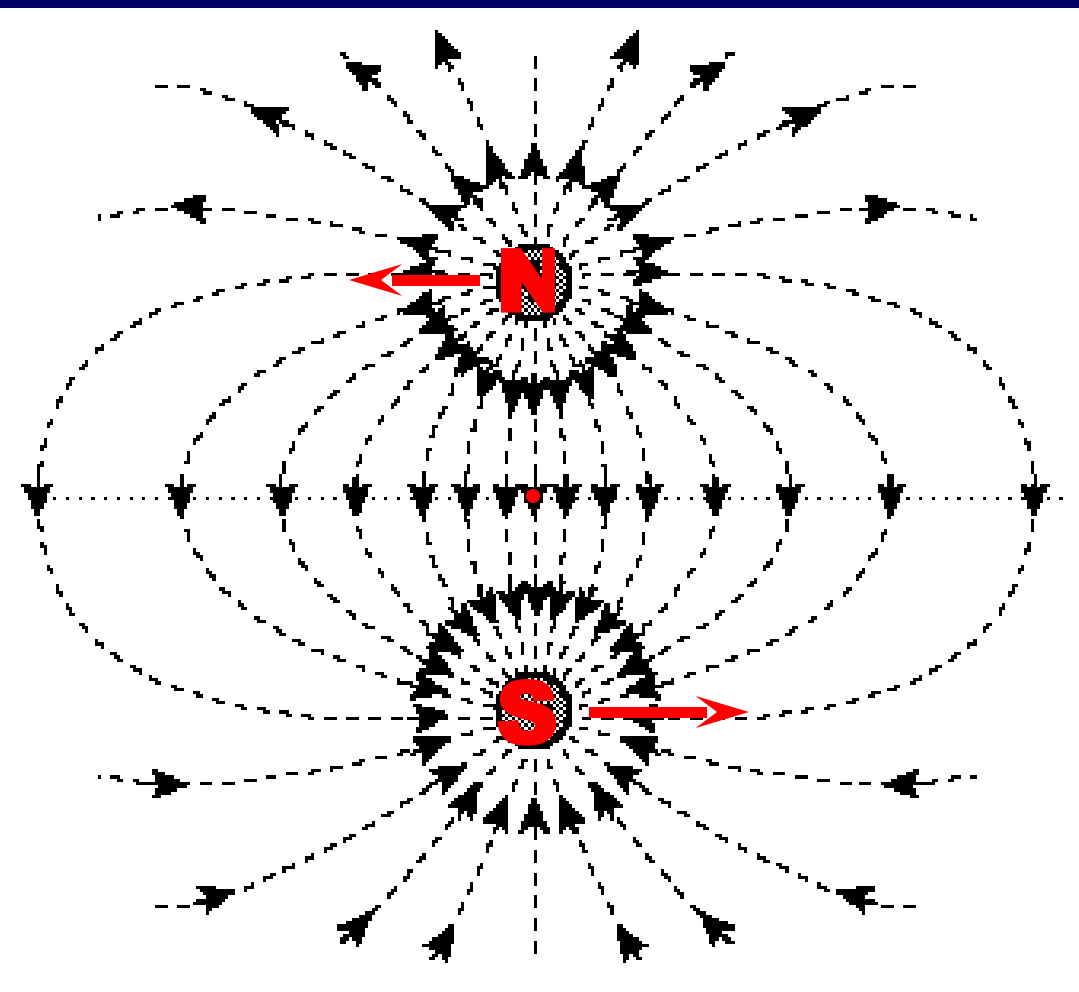
Ellipsoidal Universe Can Solve the Cosmic Microwave Background Quadrupole Problem

L. Campanelli,^{1,2,*} R. Cea,^{3,4,†} and L. Tedesco^{1,4,‡}

Учёные из Италии предположили, что Вселенная может иметь вытянутую, а не правильную сферическую, форму. Вселенная могла растянуться в эллипсоид под действием магнитного поля, распределенного по ней, или из-за дефектов в структуре пространства-времени. Предположение было сделано на основе данных, собранных космическим аппаратом NASA WMAP.



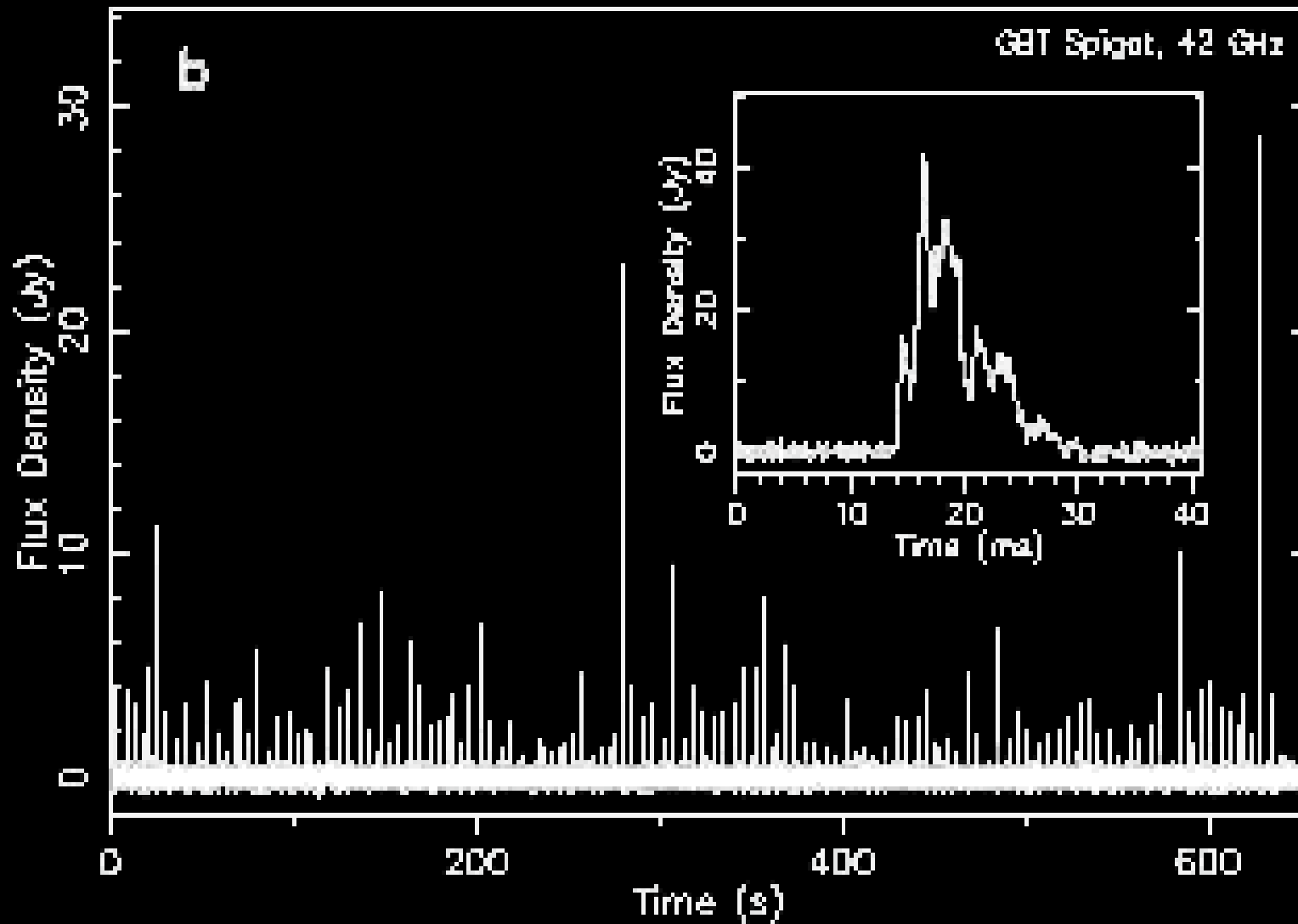
Двойная система – два входа в магнитный тоннель



- $E = GM^2/(2d)$
- $T = \pi d^{3/2}/(GM)^{1/2}$
- $V = [GM/(2d)]^{1/2}$
- $-dE/dt = 2^5 G^3 M^4 / (3c^3 d^5) + + 2^9 G^4 M^5 / (5c^5 d^5)$
- $t_{em} = E / (-dE/dt)$
- $d = [2^6 G^2 M^2 t_{em} / (3c^3)]^{1/3}$
- $T = [2^6 \pi^2 G M t_{em} / (3c^3)]^{1/2}$
- $E_{cr} = (v/c) H_0 = 4.4 * 10^{13}$
- $M_{cr} = [3c^{21} / (2^3 G^8 t_{em} E_{cr}^6)]^{1/5}$
- $T_{em} = 13 * 10^9$ лет,
 $M_{cr} = 160 M_{\odot}$

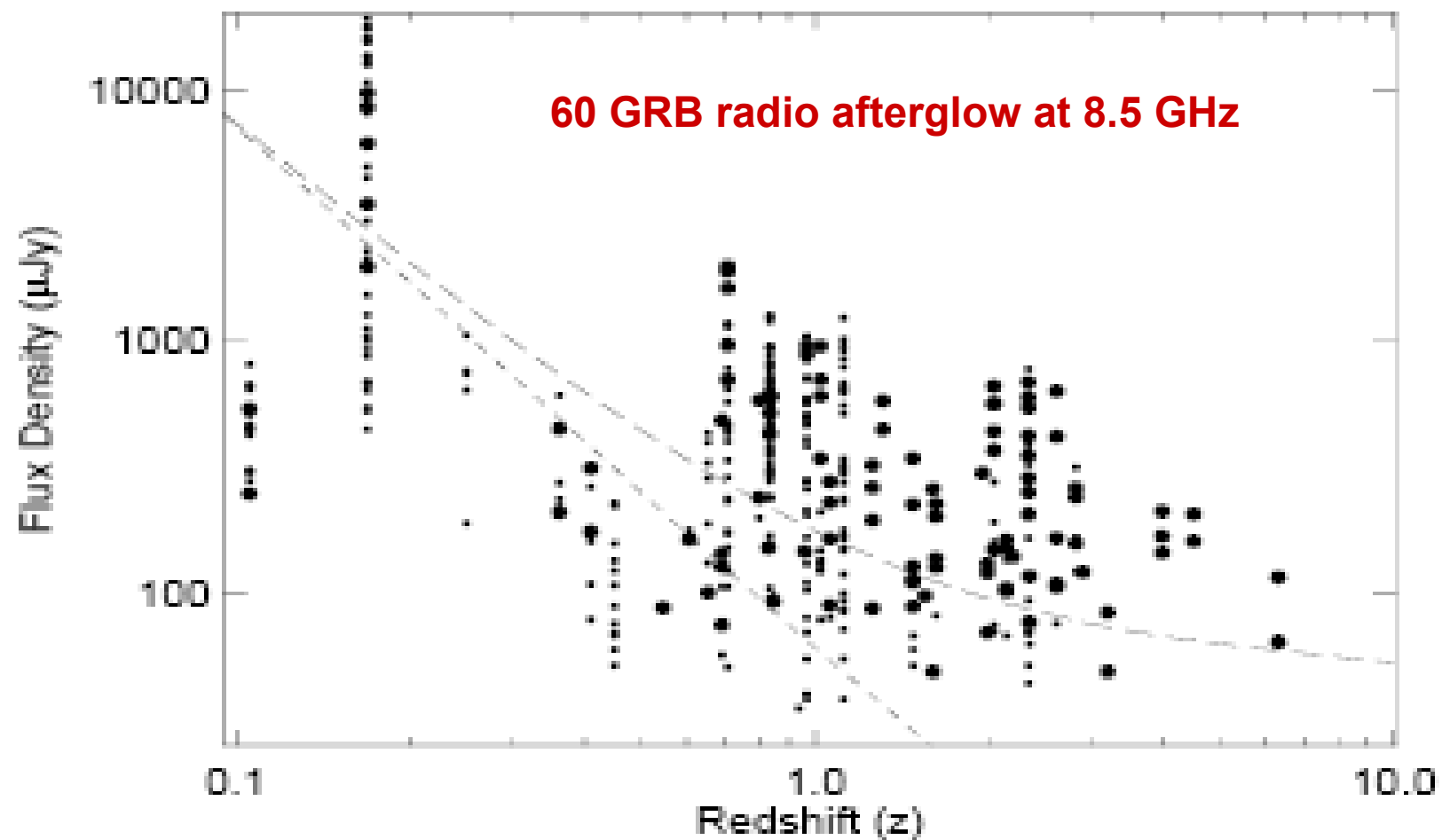
(XTE J1810-197, distance 3.5 kpc, $p=5.54$ s, DM=178 cm $^{-3}$ pc.)**Transient pulsed radio emission from a magnetar**

Fernando Camilo ¹, Scott M. Ransom ², Jules P. Halpern ¹, John Reynolds ³, David J. Helfand ¹, Neil Zimmerman ⁴ & John Sarkissian ³



AN ENERGETIC AFTERGLOW FROM A DISTANT STELLAR EXPLOSION

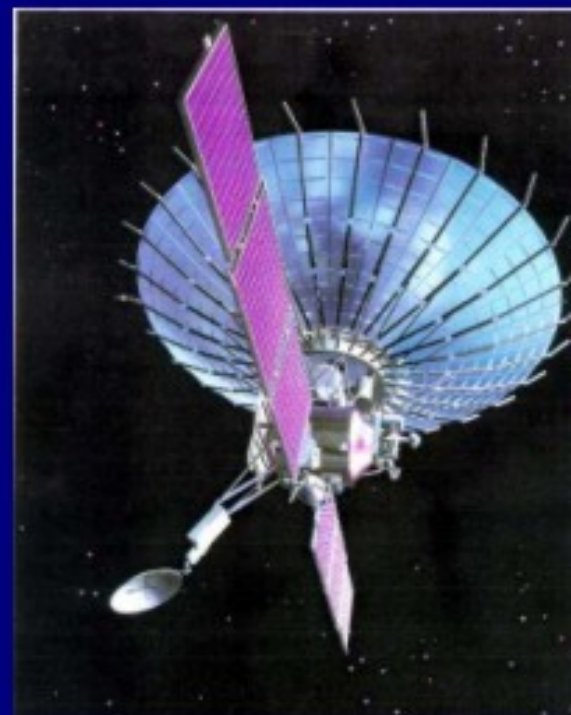
D. A. FRAIL,¹ P. B. CAMERON,² M. KASLIWAL,² E. NAKAR,³ P. A. PRICE,⁴ E. BERGER,^{5,6,7} A. GAL-YAM,^{2,7} S. R. KULKARNI,²



Imagine a picture of Einstein is moving very slowly behind a Schwarzschild black hole. (Original movie by Daniel Weiskopf)



Основные
параметры
МИССИИ
РАДИОАСТРОН



Диапазон (λ , см)	92	18	6,2	1,2-1,7
Ширина диапазона ($\Delta\nu$, МГц)	4	32	32	32
Ширина интерференционного лепестка (мксек дуги) при базе 350 000 км.	540	106	37	7,1-10
Чувствительность по потоку (σ , мЯн), на земле антена EVLA, 300 с. накопление	10	1,3	1,4	3,2

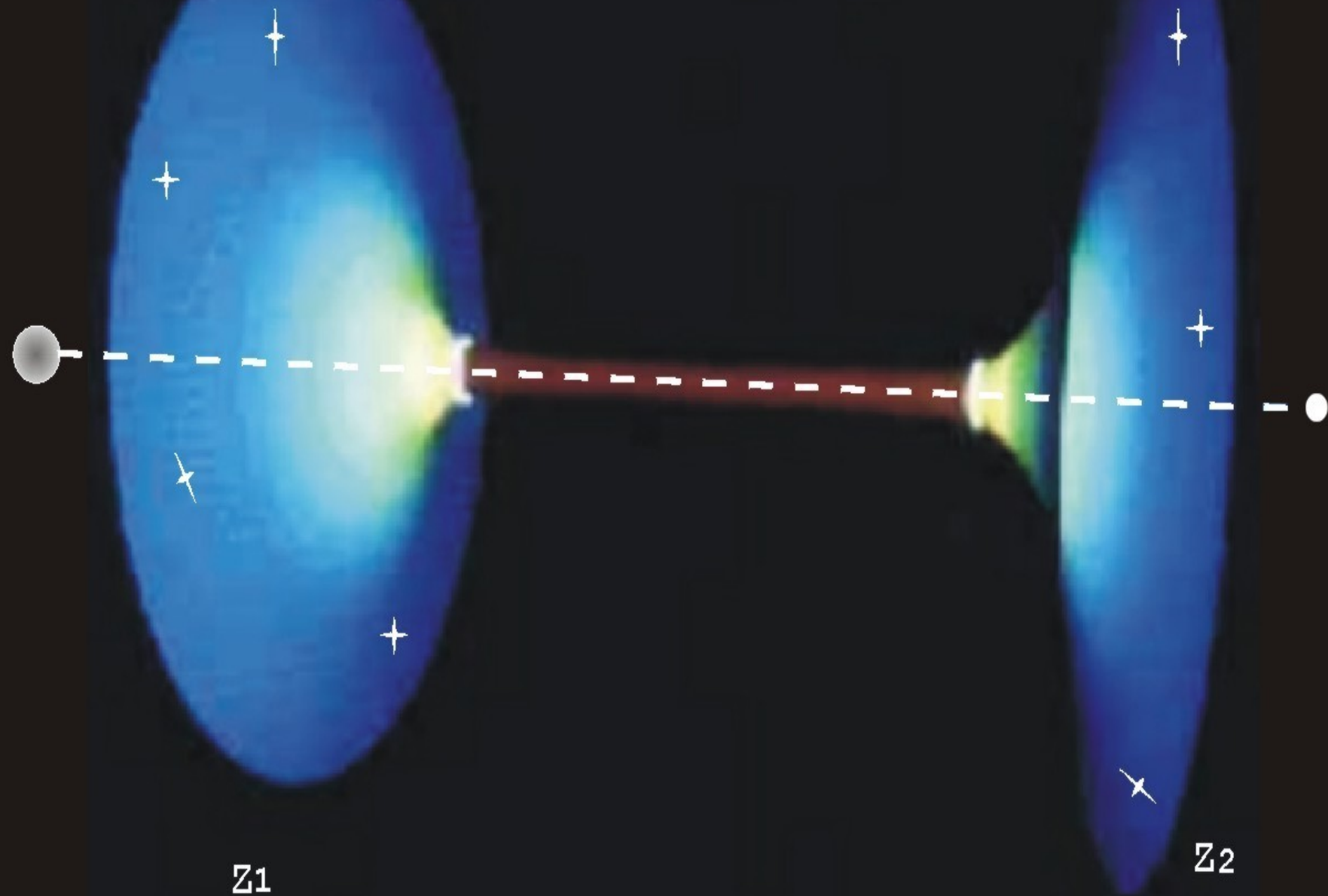
Двойные системы входов в магнитный тоннель

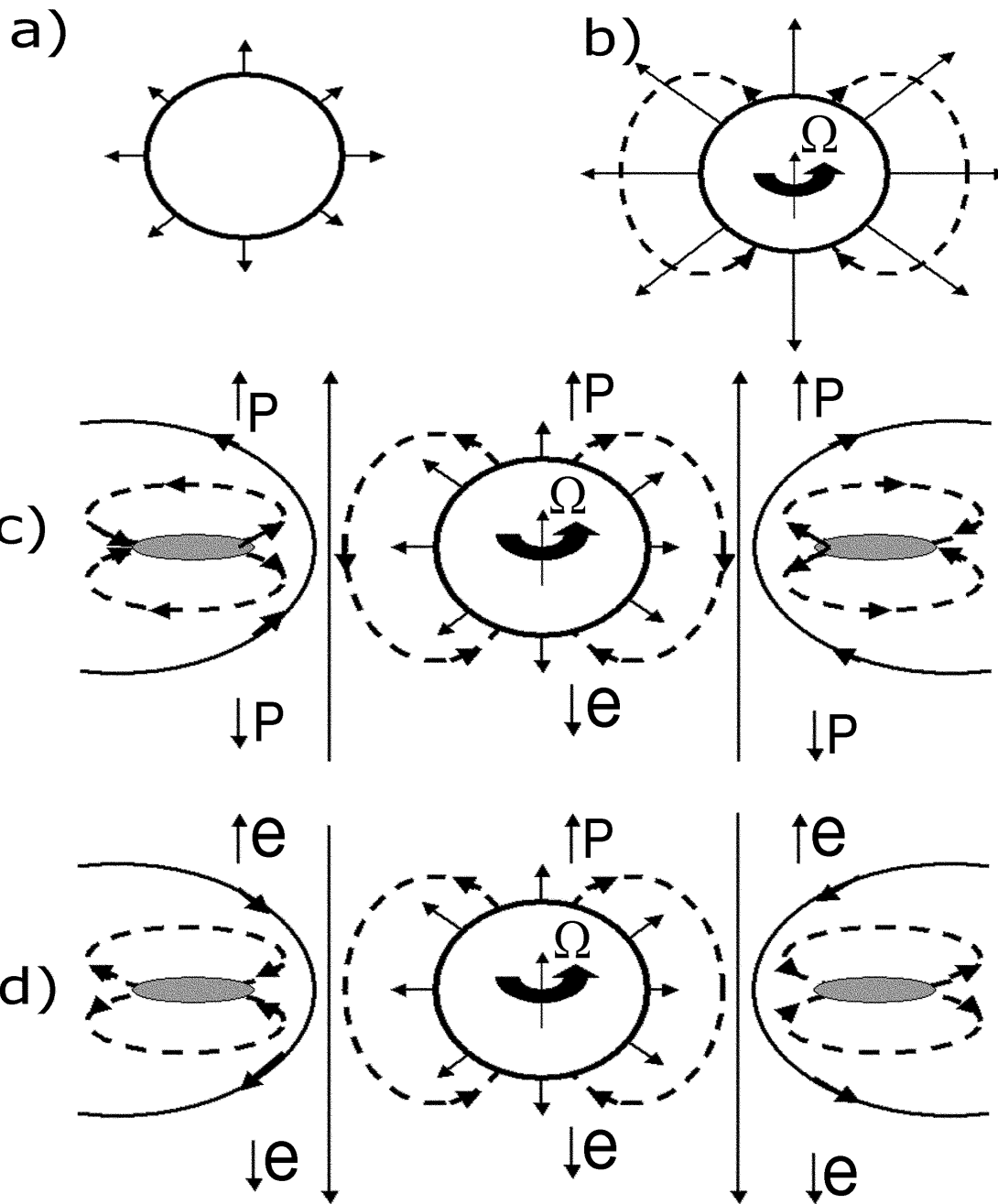
$M=2M_0$ (г)	Mc^2 (эрг)	E (эрг)	$-(dE/dt)_{em}$ (эрг/сек)	d (см)	T (сек)
$6 \cdot 10^{42}$ $(3 \cdot 10^9 M_\odot)$	$5.4 \cdot 10^{61}$	$3.2 \cdot 10^{58}$	$8.0 \cdot 10^{40}$	$3.7 \cdot 10^{19}$	$1.1 \cdot 10^{12}$
$3.2 \cdot 10^{35}$ $(160 M_\odot)$	$2.9 \cdot 10^{56}$	$6.6 \cdot 10^{48}$	$1.7 \cdot 10^{31}$	$5.2 \cdot 10^{14}$	$2.6 \cdot 10^8$
$2 \cdot 10^{33}$ $(1 M_\odot)$	$1.8 \cdot 10^{54}$	$7.4 \cdot 10^{45}$	$1.8 \cdot 10^{28}$	$1.8 \cdot 10^{13}$	$2.0 \cdot 10^7$
$4.8 \cdot 10^{18}$	$4.3 \cdot 10^{39}$	$2.4 \cdot 10^{26}$	$5.9 \cdot 10^8$	$3.2 \cdot 10^3$	1
$1.8 \cdot 10^3$	$1.6 \cdot 10^{24}$	$6.4 \cdot 10^5$	$1.6 \cdot 10^{-12}$	$1.7 \cdot 10^{-7}$	$1.9 \cdot 10^{-8}$

Тоннель с вращением
(одинаковое или противоположное)
эргосфера входа



Пролет и колебания

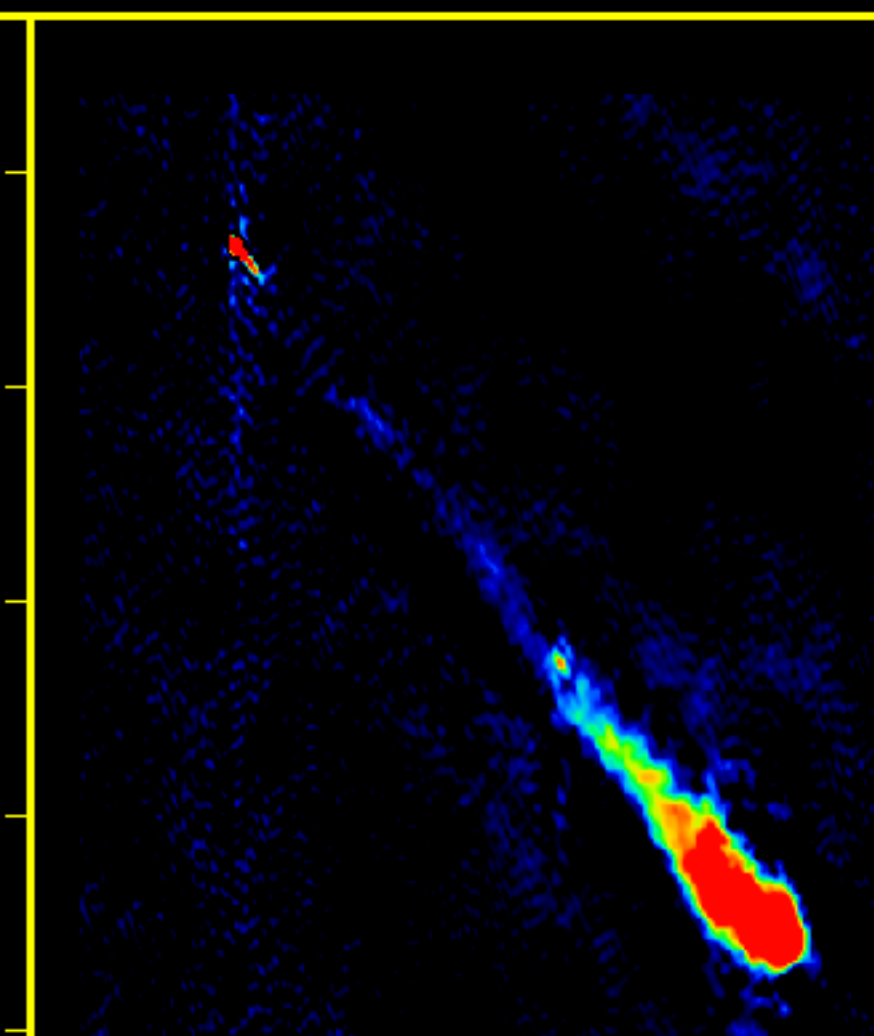
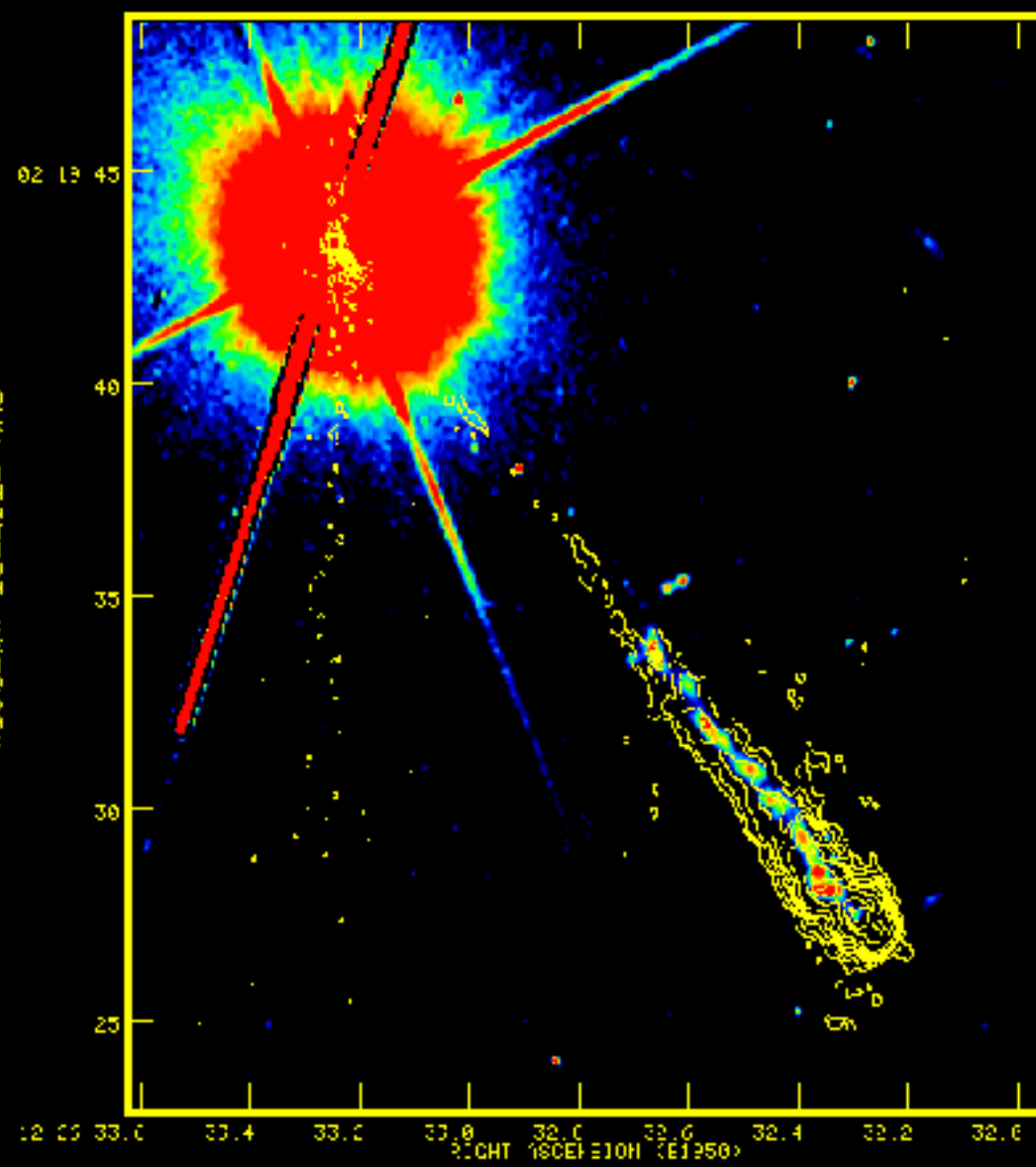


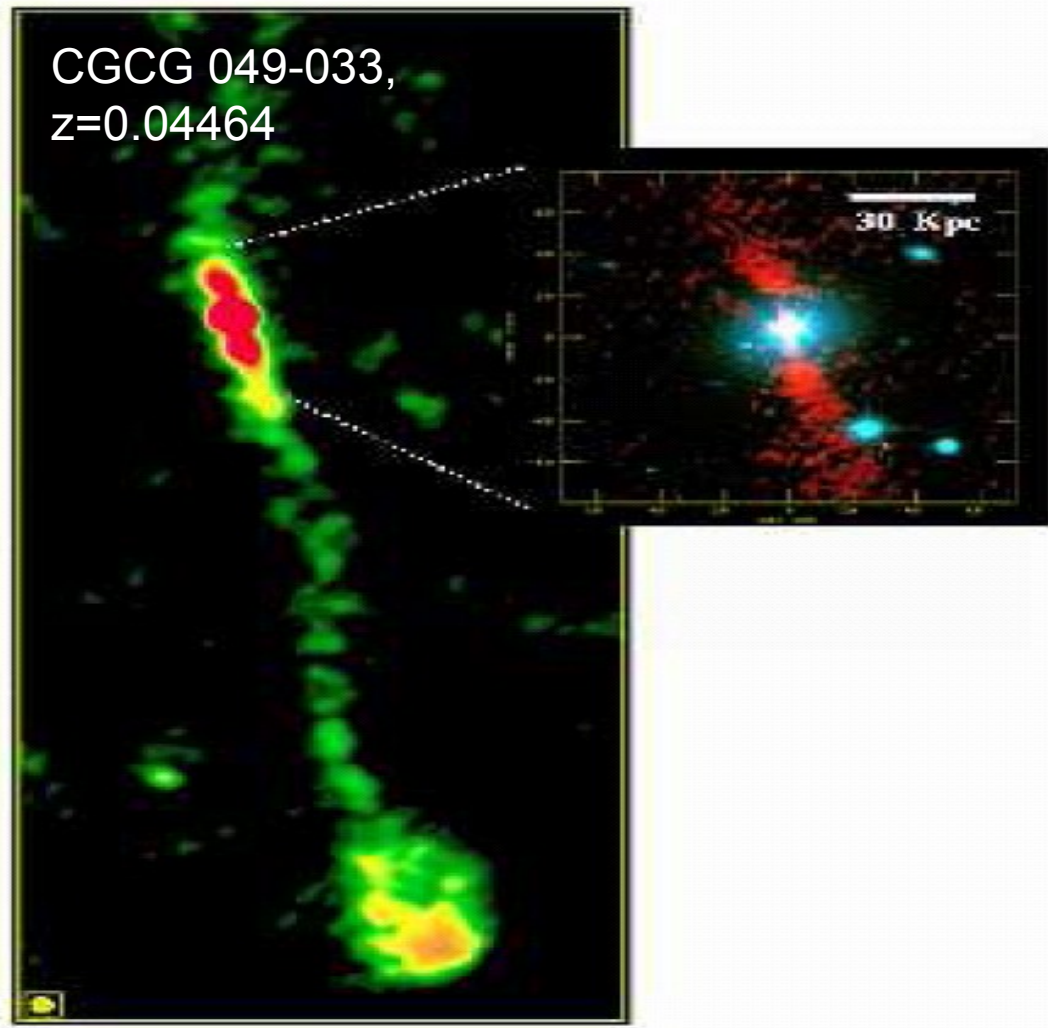
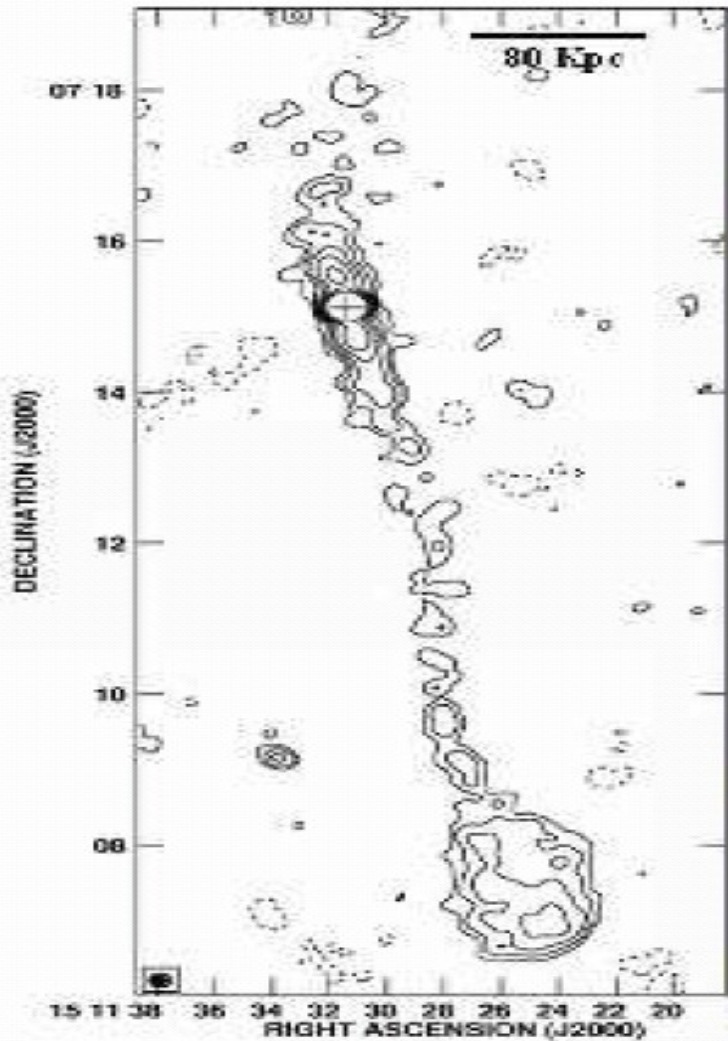


3C273

HST WFC2 / MERLIN

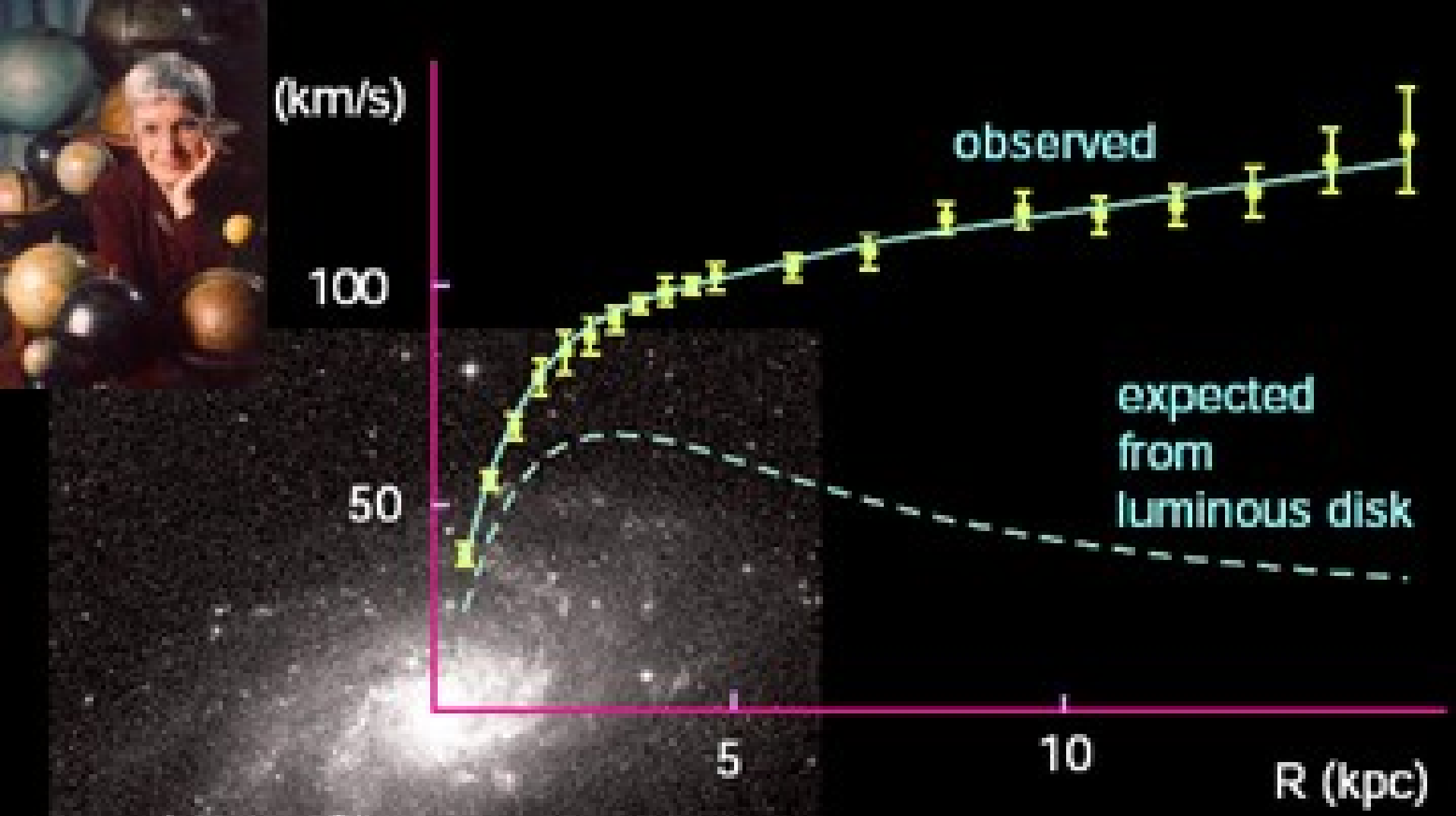
MERLIN 18cm





A giant radio jet ejected by an ultramassive black hole in a single-lobed radio galaxy,
Joydeep Bagchi, Gopal-Krishna, Marita Krause, Santosh Joshi, astro-ph 0712.0543.

Fig. 1.— GMRT maps at 1.28 GHz, showing (*left*): Intensity contours: -0.18, 0.18, 0.36, 0.72, 1.44, 3 and 6 mJy/beam; rms noise: $\sim 60 \mu\text{Jy}/\text{beam}$, and the pseudo-color image (*center*), both with a 11'' beam. The details of the inner $\sim 2'$ region (*inset*) are visible in the 3'' resolution 1.28 GHz GMRT image (shown in red) overlaid on the optical *r*-band SDSS image (shown in blue).



M33 rotation curve
(fig. 1)

A View through Faraday's Fog: Parsec-Scale Rotation Measures in Active Galactic Nuclei, **Zavala, R. T.; Taylor, G. B.**,
The Astrophysical Journal, V. 589, pp. 126-146, 2003.
BL Lac, z=0.07, F₁₅=3.23 Jy.

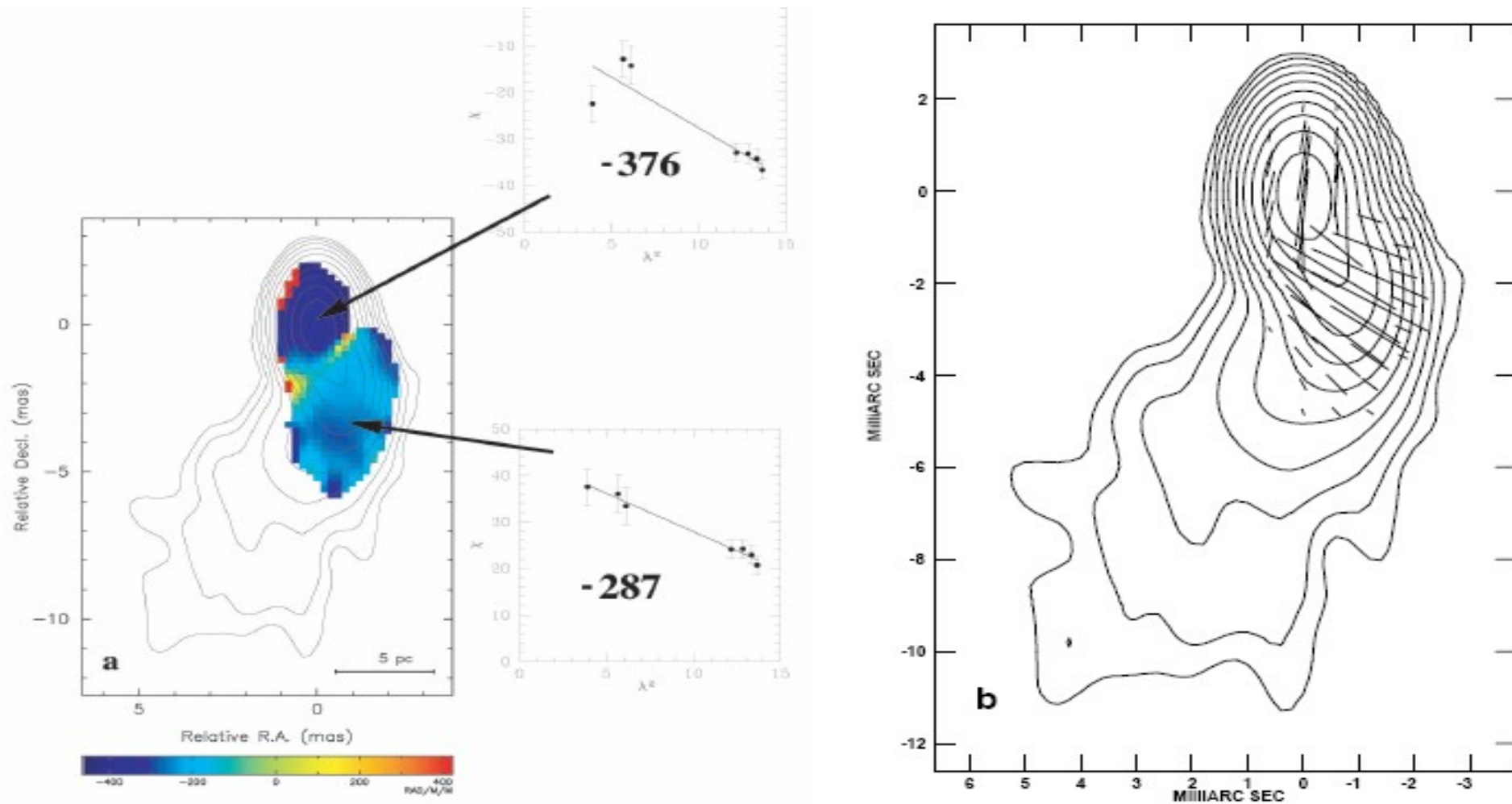


FIG. 25.—(a) RM image (color) for BL Lac overlaid on Stokes I contours at 15 GHz. The insets show plots of EVPA χ (degrees) vs. λ^2 (units of cm⁻²). (b) Electric vectors (1 mas = 25 mJy beam⁻¹ polarized flux density) corrected for Faraday rotation overlaid on Stokes I contours. Contours start at 2.2 mJy beam⁻¹ and increase by factors of 2.

A View through Faraday's Fog. II. Parsec-Scale Rotation Measures
in 40 Active Galactic Nuclei,
Zavala, R. T.; Taylor, G. B.,
The Astrophysical Journal, V. 612, pp. 749-779, 2004.
BL/Q 3C446, z=1.40, F₁₅=3.92 Jy.

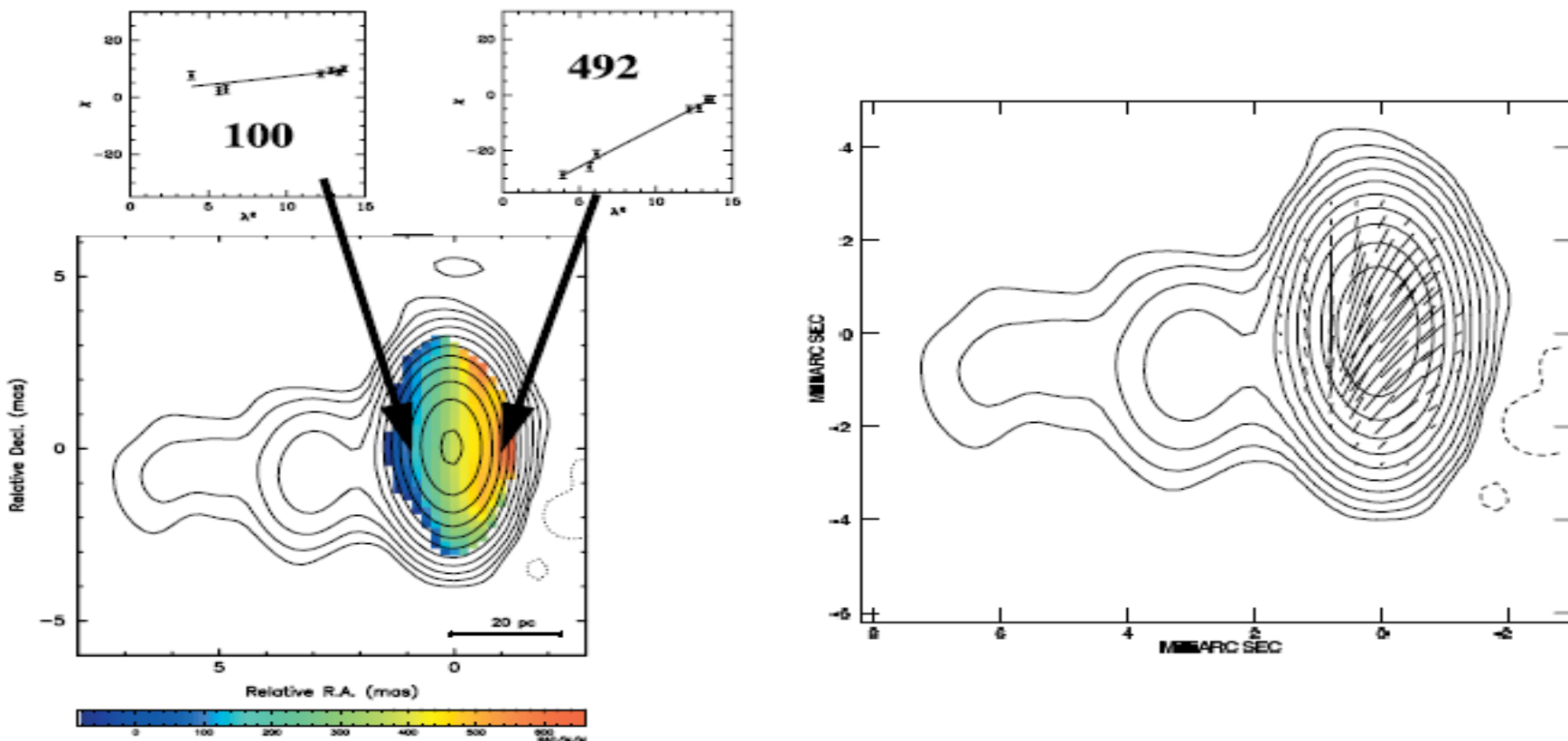
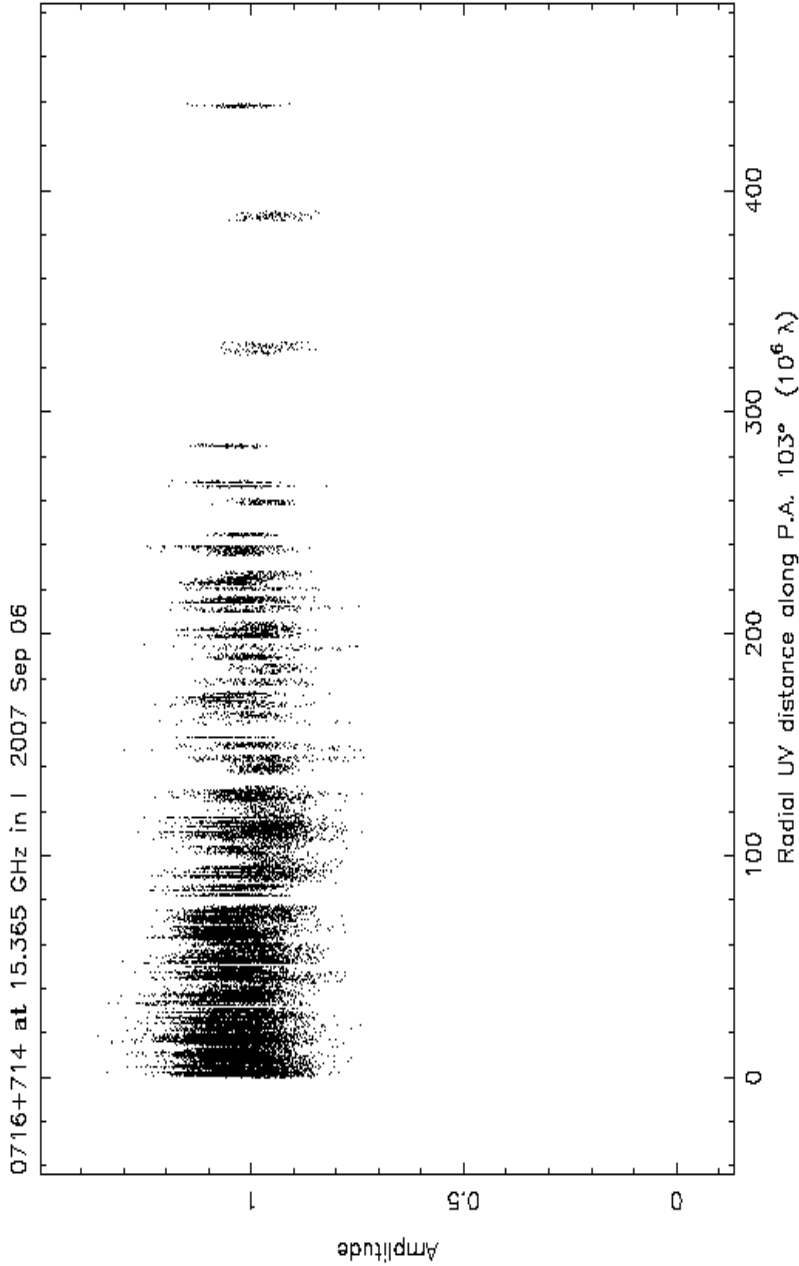
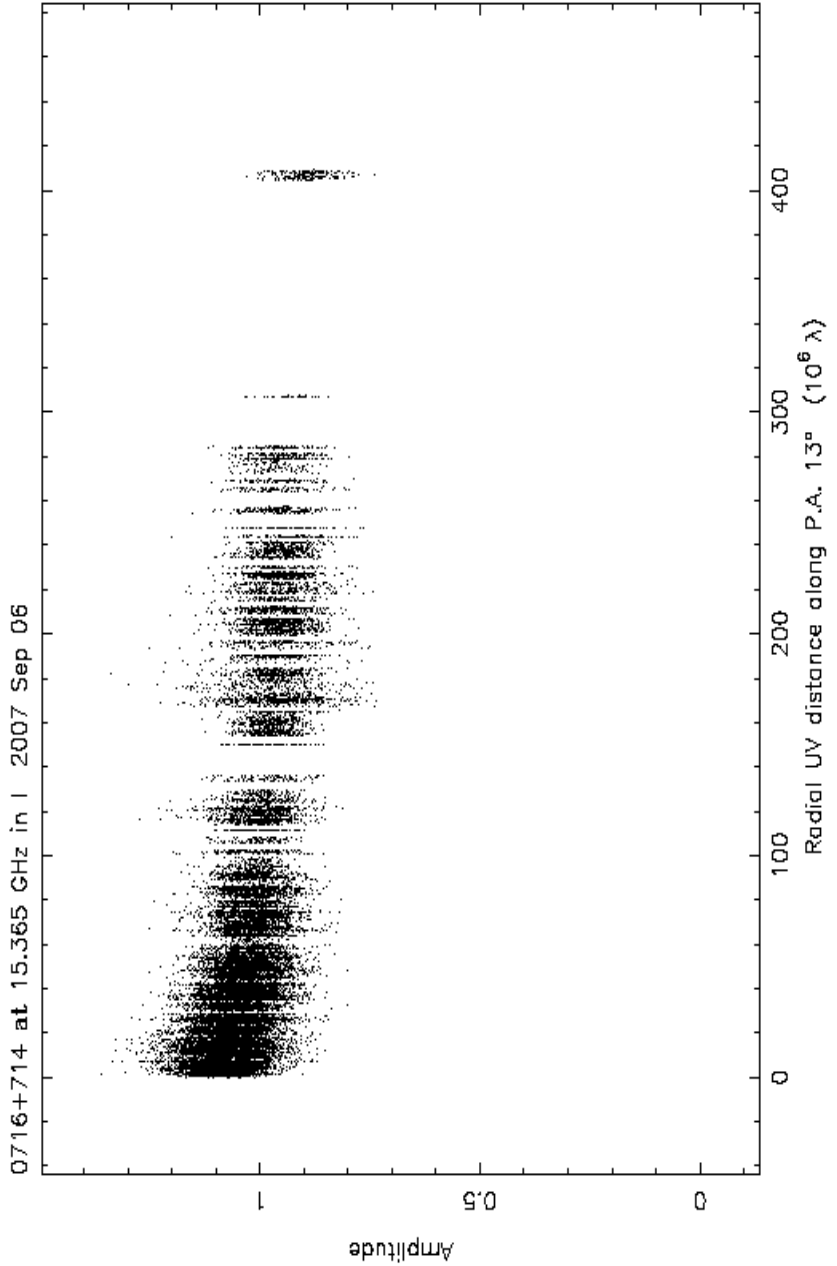


FIG. 3.3.—Left: RM image (color) for 3C 446 overlaid on Stokes I contours at 15 GHz. The inset is a plot of EVPA χ (degrees) vs. λ^2 (cm^2). Right: Electric vectors (1 mas = 200 mJy beam $^{-1}$ polarized flux density) corrected for Faraday rotation overlaid on Stokes I contours. Contours start at 5.1 mJy beam $^{-1}$ and increase by factors of 2.

Jet par

0716+714, VLBA, 2 cm

Jet perp



Left: $p=0.21$ d (5 hr). Right: $p=0.11$ and 0.23 d (2.6 and 5.5 hr).

OPTICAL MONITORING OF S5 0716+714

1823

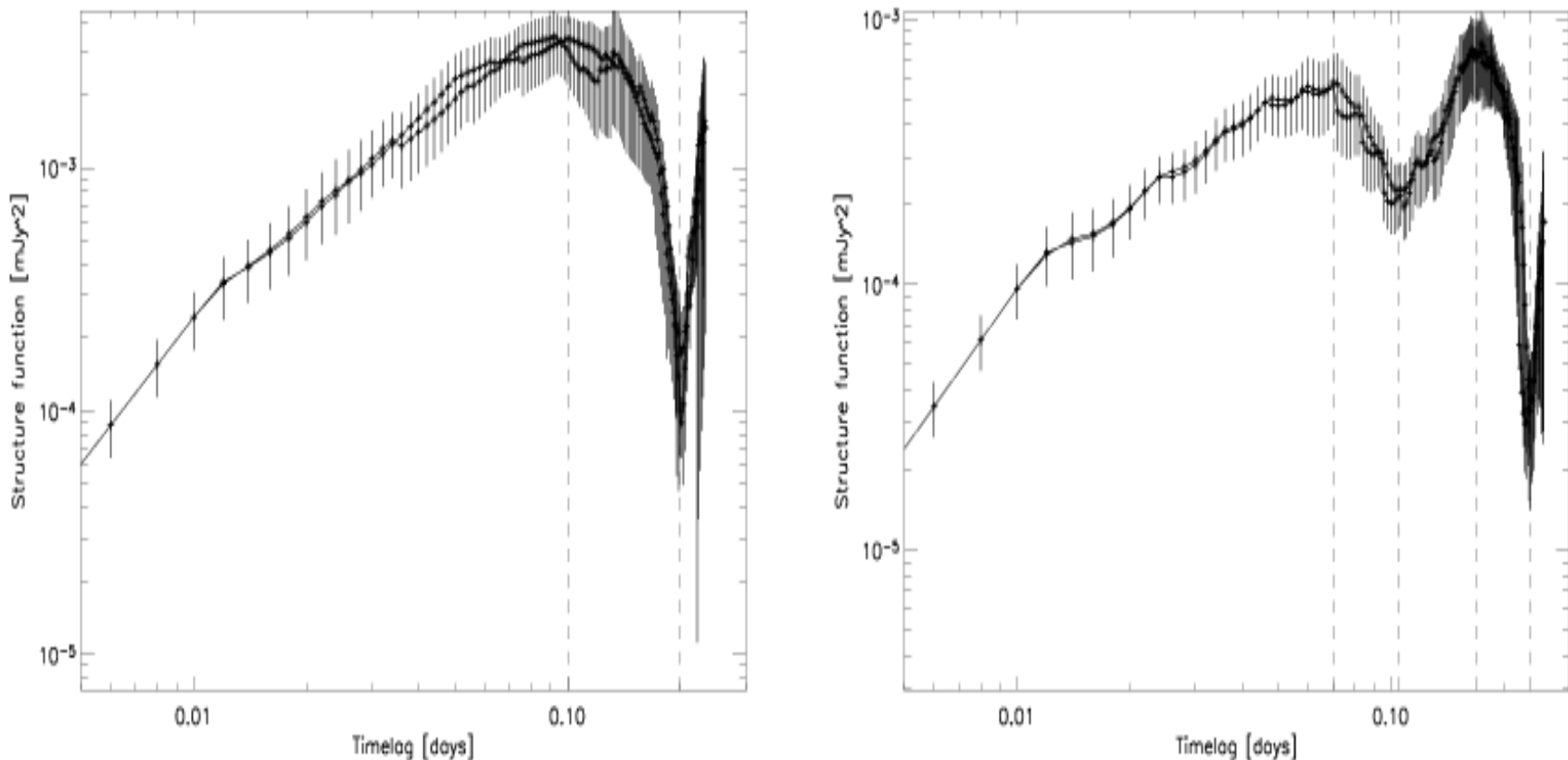


FIG. 4.—Structure function of S5 0716+714 on JD 2,453,006 (*left*) and 2,453,007 (*right*). The dashed lines indicate timescales at the maxima and periods at the minima of the structure functions.

ABSTRACT

Faraday rotation of radio source polarization provides a measure of the integrated magnetic field along the observational lines of sight. We compare a new, large sample of Faraday rotation measures (RMs) of polarized extragalactic sources with galaxy counts in Hercules and Perseus-Pisces, two nearby superclusters. We find that the average of RMs in these two supercluster areas are larger than in control areas in the same galactic latitude range. This is the first RM detection of magnetic fields that pervade a supercluster volume, in which case the fields are at least partially coherent over several megaparsecs. Even the most conservative interpretation of our observations, according to which Milky Way RM variations mimic the background supercluster galaxy overdensities, puts constraints on the IGM magneto-ionic "strength" in these two superclusters. We obtain an approximate typical upper limit on the field strength of about $\sim 0.3 \mu\text{G} \text{ kpc}/(500 \text{ kpc})$, when we combine our RM data with fiducial estimates of electron density from the environments of giant radio galaxies, and of the warm-hot intergalactic medium (WHIM).

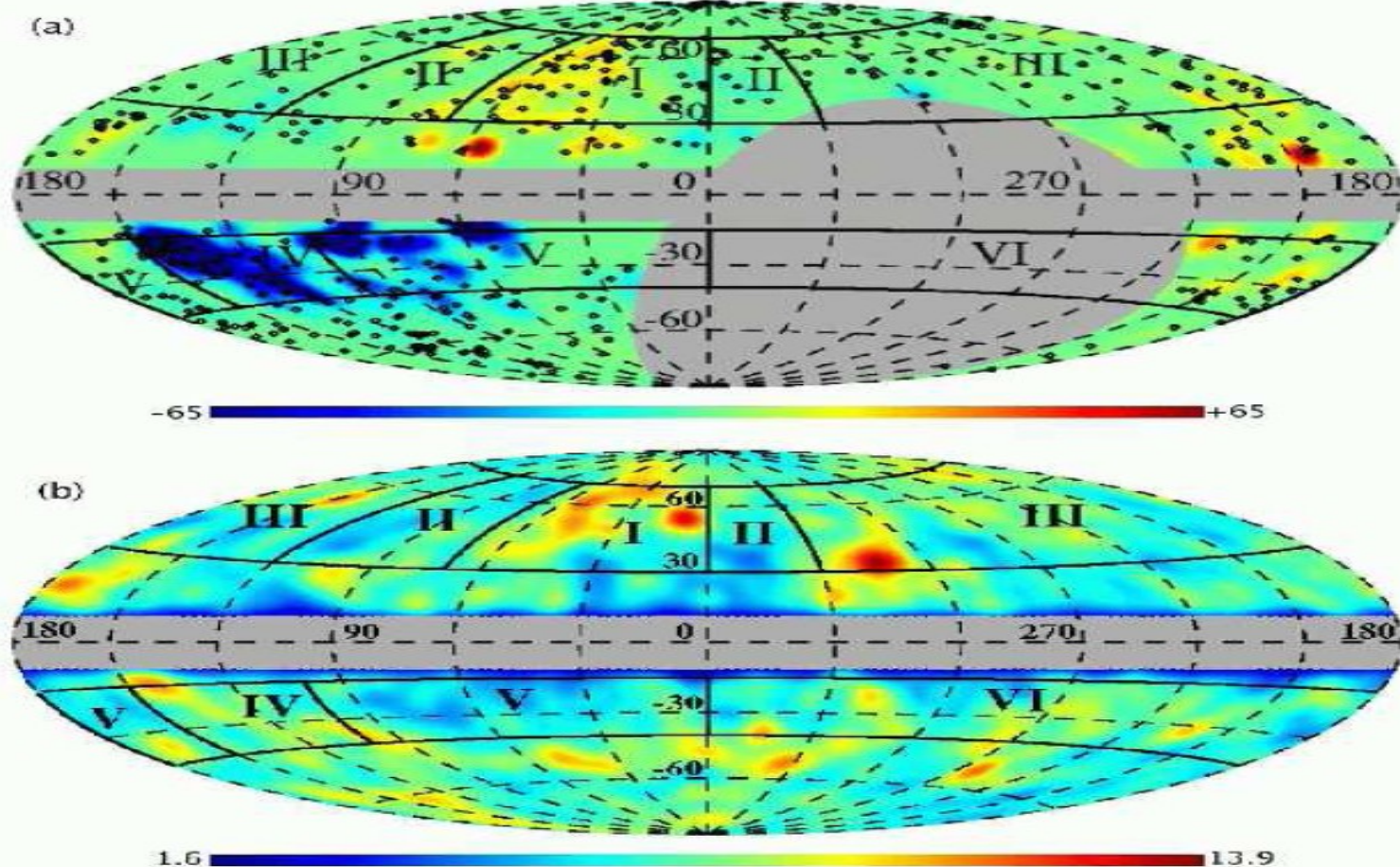


FIG. 1.— (a) All-sky plot of the extragalactic source SRM distribution. The square black points show the positions of individual SRM sources. The color map shows SRM variations Gaussian-smoothed to 7 degrees in an Aitoff projection of galactic coordinates. The color range from blue to red signifies a range of SRM values from -65 rad m^{-2} to 65 rad m^{-2} . The excluded areas (see text) are for $|b| > 25^\circ$ and $\delta \leq -25^\circ$ (b) The 2MASS galaxy column density Gaussian-smoothed to 7 degrees in the same coordinates as in (a). The Hercules and Perseus-Pisces superclusters lie in the high density parts labeled I and IV, respectively. Labels II, III and V indicate the RM comparison zones (see subsection 3.1, and table 1).

**astro-ph/0411687 , The Galactic Centre region, Subhashis Roy,
Bull.Astron.Soc.India, 32, 205-213, 2004.**

Abstract. We have observed the central $45'$ region of the Galaxy at 620 MHz band of the Giant Metrewave Radio Telescope (GMRT) in radio continuum, and measured the polarisation properties of 64 small diameter background extragalactic sources seen through the $-6^\circ < l < 6^\circ$, $-2^\circ < b < 2^\circ$ region with the Australia Telescope Compact Array (ATCA) and the Very Large Array (VLA). Our 620 MHz observations show that Sgr A* is located behind the HII region Sgr A West. Using the ATCA and the VLA observations, we measured the Faraday rotation measure (RM) of the polarised sources. The measured RMs are mostly positive, and show no reversal of sign across the rotation axis of the Galaxy. This rules out any circularly symmetric model of magnetic field in the region. We estimate the magnetic field strength in the region to be $\sim 10 \mu\text{G}$, which raises doubts against an all pervasive mG field in the central few hundred pc of the Galaxy.

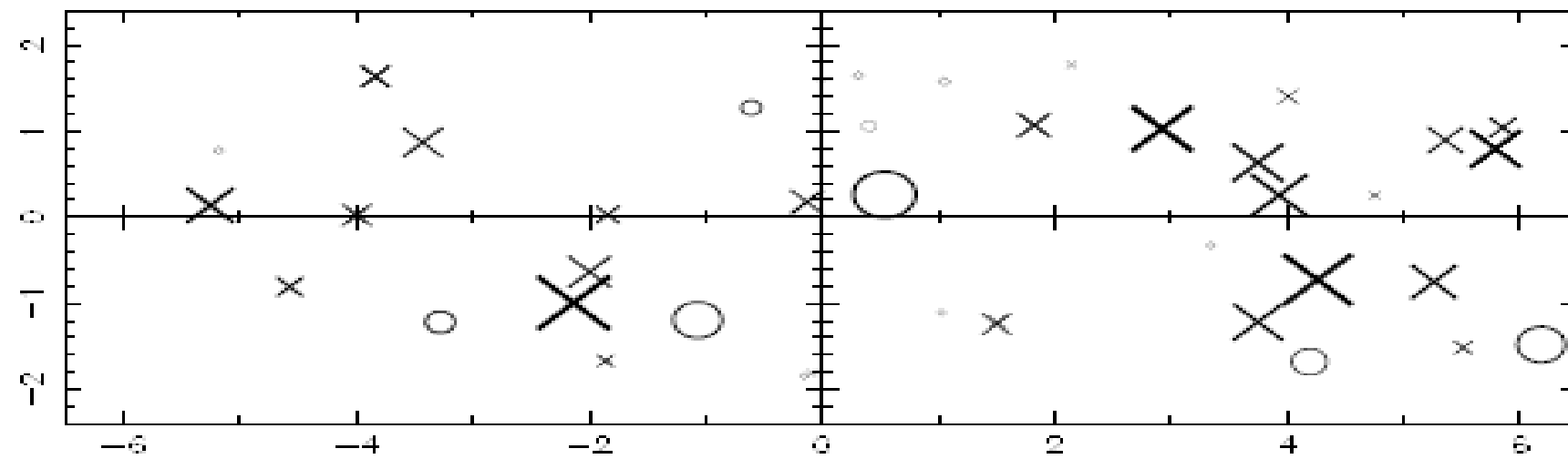


Figure 5. The plot of the RM towards various sources as a function of the Galactic longitude and latitude. The cross symbol (\times) indicates positive RM and the circle (\circ) negative RMs, where the symbol size increases linearly with $|\text{RM}|$.

gives rise to the bisymmetric spiral configuration of the magnetic field in galaxies. In our Galaxy, the magnetic field configuration has been suspected to be bisymmetric (Simard-Normandin & Kronberg 1980), in which case, the field does not undergo a reversal of sign across the centre. Our observations support the bisymmetric spiral configuration in the inner parts of our Galaxy.

Faraday Rotation Measures in the Parsec-Scale Jets of the Radio Galaxies M87, 3C 111, and 3C 120, Zavala, R. T., Taylor, G. B., The Astrophysical Journal, Volume 566, Issue 1, pp. L9-L12, 2002.

M87

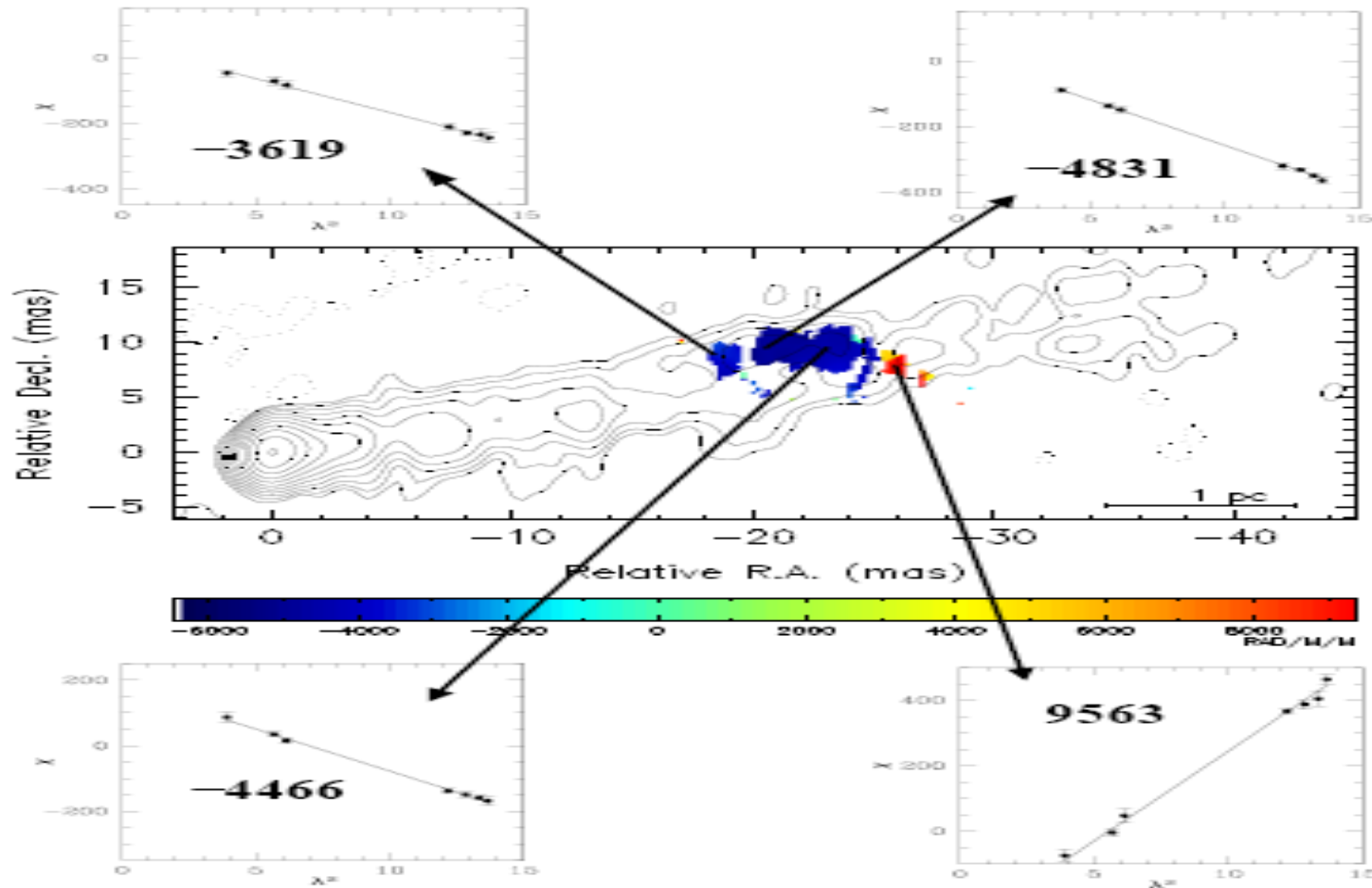
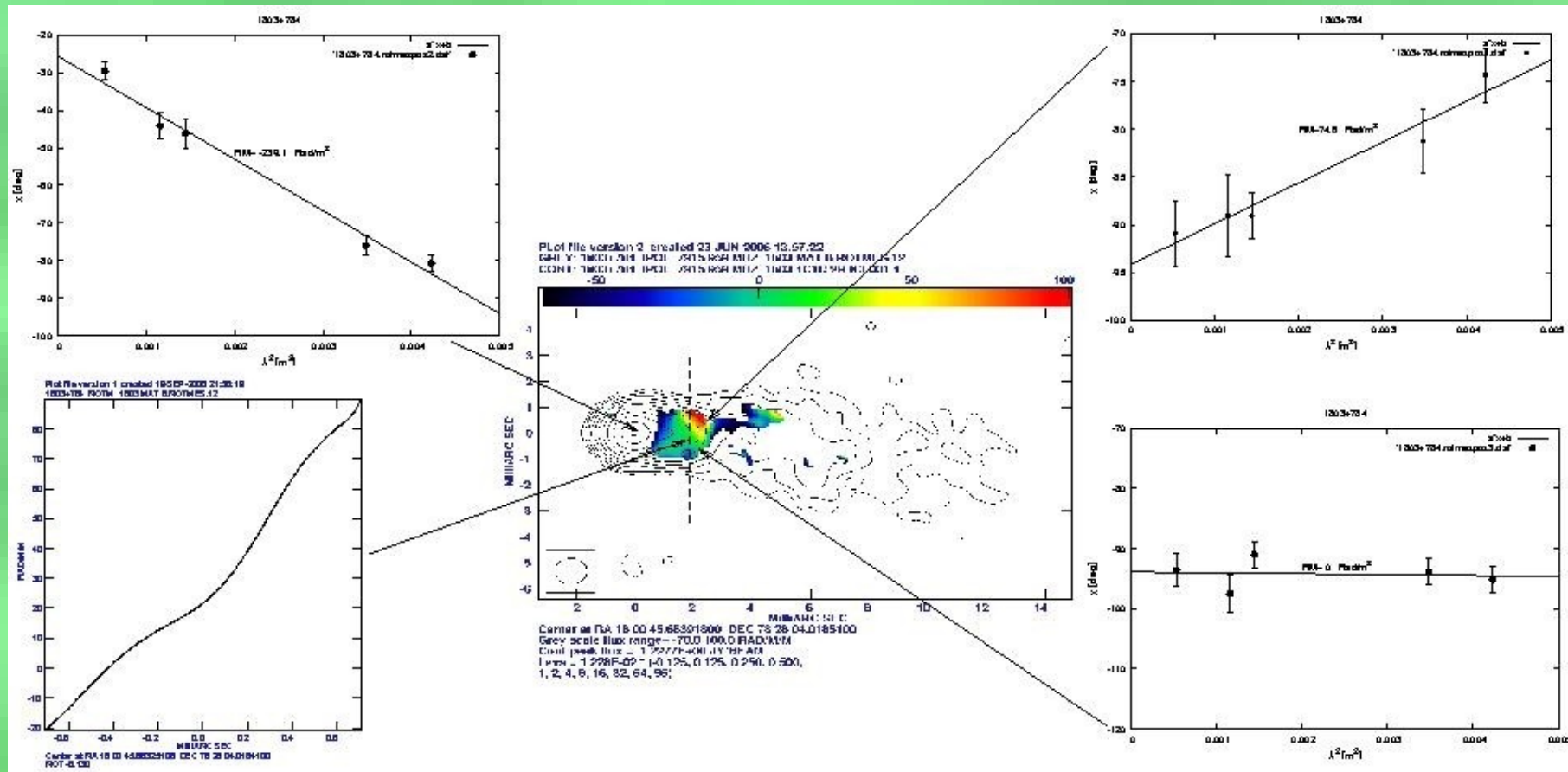


Fig. 2.— RM image of M87 from data at 8 to 15 GHz, with contours of total intensity at 8 GHz overlaid. The restoring beam has dimensions 1.0×2.7 milliarcsec at position angle 0° . The colorbar ranges from -6300 to $+9300$ rad m⁻². Contours start at 1 mJy/beam and increase by factors of 2.

Detection of transverse gradients in 1803+784,M. Mahmud, D. Gabuzda, 2006.

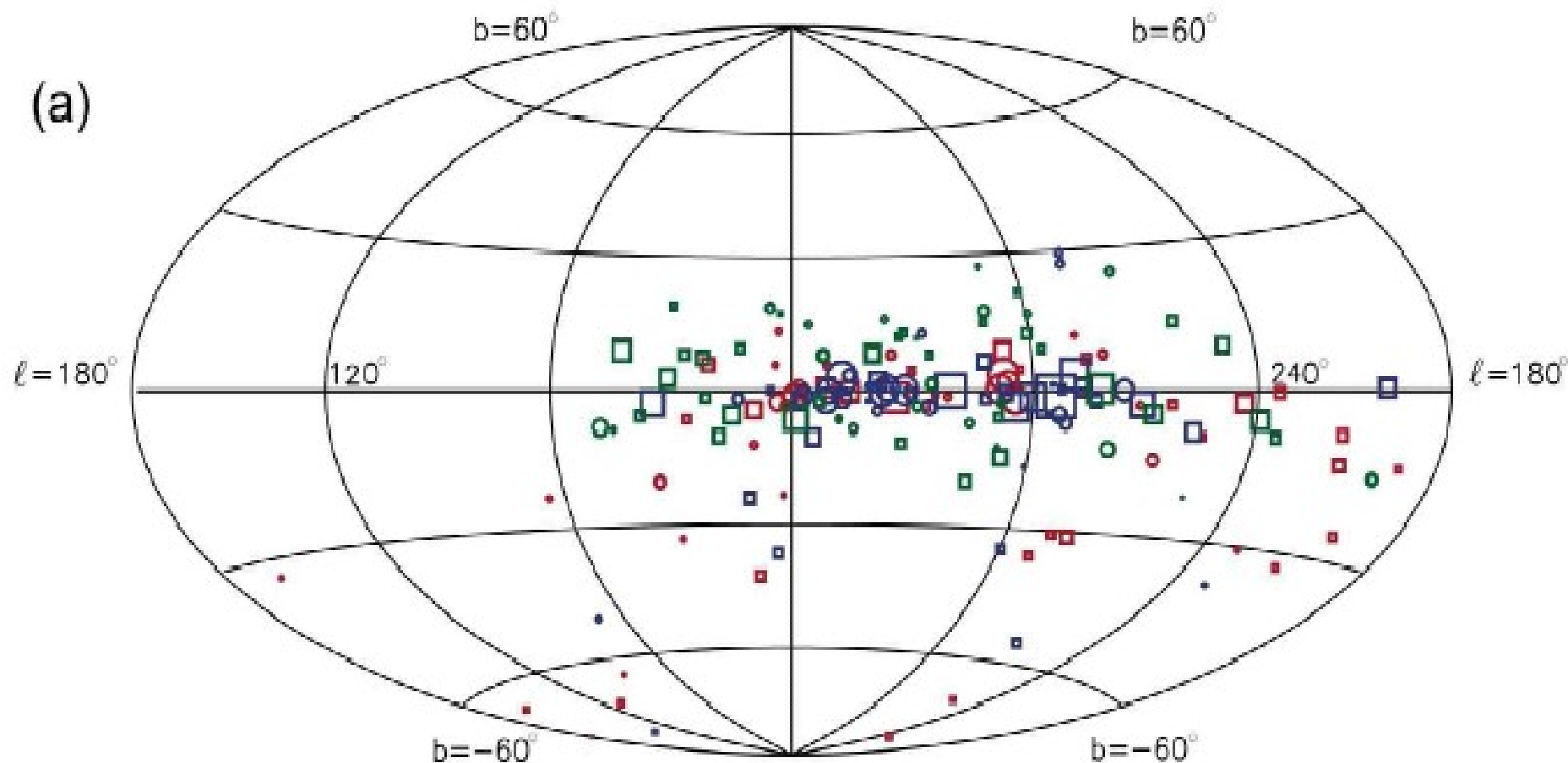


- North-South RM gradient at ~ 2 mas from core.
- Hints of transverse RM gradient further along jet (at ~ 5 mas).
- Direction of North-South gradient reversed as compared to Zavala and Taylor (2003)
- Possible explanation: Kink in magnetic field followed by reconnection.

New pulsar rotation measures and the Galactic magnetic field, Noutsos, A., Johnston, S., Kramer, M., Karastergiou, A., arXiv0803.0677.

150 pulsar Rotation Measures (RMs) using the 20-cm receiver of the Parkes 64-m radio telescope.

(a)



46 Unpublished RMs

49 Revision to RMs by Han et al. (2006)

55 Revision to RMs by others

○ 69 negative RMs

□ 81 positive RMs